PHYSICAL REVIEW
LETTERS

VOLUME 7 OCTOBER 15, 1961 NUMBER 8

# SPECIFIC HEAT OF $He^3$ UNDER PRESSURE*

A. C. Anderson,† G. L. Salinger, W. A. Steyert, and J. C. Wheatley‡
Department of Physics, University of Illinois, Urbana, Illinois
(Received July 28, 1961; revised manuscript received September 19, 1961)

We have measured the heat capacity of a mixture of $He^3$ and powdered cerium magnesium nitrate (CMN) from 0.02°K to temperatures as high as 0.1°K at pressures of 0.12, 1.10, 3.4, 6.1, 11.8, 21.1, and 28.0 atm and for pressures greater than that of the minimum in the melting curve, $P_{min}$, at external pressures of 30.7, 32.8, and 34.8 atm. The specific heat seems to be linear in $T$ below temperatures of about 0.03°K only at the lowest pressures, but at higher pressures it is possible that the linear temperature dependence of the specific heat characteristic of a Fermi liquid has not been developed by 0.02°K. Assuming a Fermi liquid behavior at 0.03°K, we obtain at zero pressure a ratio of the specific heat to temperature which is considerably greater than that deduced from earlier experiments[1-3] and predicted by Brueckner and Gammel,[4] but in agreement with the theory of Goldstein.[5] We also deduce a lower limit for the isobaric expansion coefficient. We find no discontinuity in specific heat down to 0.02°K for the full pressure range in the liquid although the theories[6,7] of cooperative transitions in $He^3$ predict an increasing transition temperature with effective mass and hence with pressure. We find that the liquid phase of $He^3$ at pressures above $P_{min}$ and at low temperatures has a smaller specific heat and a reduced thermal boundary resistance relative to that at somewhat lower pressures. We were able to measure the thermal boundary resistance at various pressures in a more restricted temperature range than the specific heat and found that it decreased slowly as pressure increased. Details of these measurements will be given in a subsequent publication.

The measurements on the solid revealed a small specific heat increasing as the temperature decreased below 0.036°K, indicating that the exchange interaction is much smaller than that predicted by Bernardes and Primakoff.[8]

The cell containing the mixture of $He^3$ and CMN had the same geometry as that reported previously,[1] except that there was 0.585 g of CMN in the cell and that the heater consisted of a bifilar lead of 0.002-inch diameter manganin wire 6 inches long, the ends of which were silver soldered to 0.004-inch diameter copper leads. These joints were inside the cell. The Epibond 100A[9] plug, which closed the cell, was sealed by Epibond 121 which is nonmagnetic.[10]

The magnetic susceptibility of the cell was carefully measured in the 0.3-1°K temperature range both with and without CMN inside. We were able to calibrate the thermometer to within 2% and to deduce that magnetic effects caused an error of less than 1.5%.

The pressure was applied to the $He^3$ using a stainless steel Toepler pump. The pressure was set using a dead-weight tester[11] and monitored using a Helicoid gauge.[12] The hydrostatic pressures due to mercury and oil in the pressure system were measured and corrections were applied to the dead-weight pressures. The pressure was held constant to within 1% during a run.

The quantity of $He^3$ in the cell below 1°K was measured to be $0.0080 \pm 0.0002$ mole at 0.12 atm. The $He^4$ content was less than 4 parts in $10^5$ and the tritium decay rate in the cell was less than 300 disintegrations/sec.

The low temperatures were produced in essen-

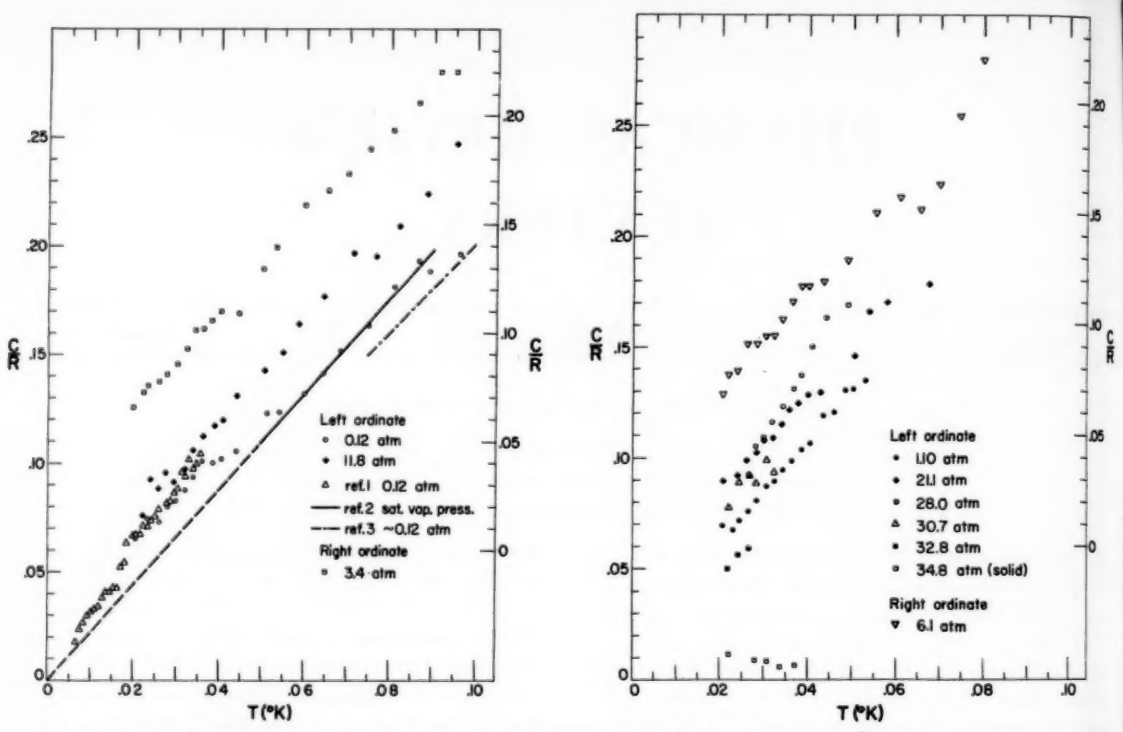


FIG. 1. Ratio of specific heat, $C$, to gas constant $R$ (=8.317 joules/mole K°) for $He^3$ under pressure. The right ordinate is displaced upward in order to display the data better. Above 29 atm, the pressures indicated were those in the external system.

tially the same way as previously described.[1,13] Temperatures down to 0.02°K were obtained when the cell was thermally coupled directly to the refrigerator using copper "coil foils."[13] Temperatures down to 0.04°K were obtained when a lead switch was inserted between the cell and the refrigerator.

The data for the heat capacity were taken by the method of reference 1. With the tight thermal coupling, the best data were obtained around 0.03°K; and with the lead switch, the best data were obtained from 0.06 to 0.08°K.

The ratio of the specific heat, $C$, to the gas constant, $R$, is displayed as a function of temperature, $T$, for various pressures in Fig. 1. In reducing the heat capacity data to $C/R$, we assumed the volume of the $He^3$ in the cell to be constant. The number of moles in the cell was determined from the molar volumes of Sherman and Edeskuty,[14] extended to 0°K by extrapolating the density data of Lee, Fairbank, and Walker[15] to 0°K and higher pressures. The molar volume ratios used for the reduction of the data are given in Table I. For pressures greater than $P_{min}$, the molar volume was assumed to be that of the liquid just before the filling tube plugged. This assumption is probably not precise, but it does not lead to errors in excess of 5% in $C/R$.

The data of reference 1, plotted on Fig. 1, have been corrected for an incorrect temperature calibration resulting from the magnetism[10] of SC-13

Table I. Density ratios of $He^3$ near $T=0$°K.

| $P$ (atm) | $\rho/\rho_{0.12}$ [a] | $P$ (atm) | $\rho/\rho_{0.12}$ [a] |
|---|---|---|---|
| 0.12 | 1.000 | 21.1 | 1.338 |
| 1.10 | 1.033 | 28.0 | 1.393 |
| 3.4 | 1.094 | 30.7 [b] | 1.422 |
| 6.1 | 1.148 | 32.8 [b] | 1.437 |
| 11.8 | 1.234 | 34.8 [b] | 1.452 |

[a] $\rho/\rho_{0.12}$ is the ratio of the density of $He^3$ at pressure $p$ to that at 0.12 atm near $T=0$°K. The molar volume of $He^3$ at 0.12 atm is 36.73 $cm^3$/mole. $\rho/\rho_{0.12}$ is used to reduce the heat capacity data to specific heats.

[b] This is the pressure at which the $He^3$ plug formed.

flexible silver micropaint[16] used to join the heater to the copper leads inside the cell. Since the same coil system and geometry were used in both reference 1 and this experiment, the temperature calibration in reference 1 was assumed to differ from the present one only by the ratio of the masses of CMN. Both the corrected calibration constant of reference 1 and that in the present experiment agree within 5% with that calculated from the known geometry, galvanometer flux sensitivity, and properties of CMN.

A lower limit on the values of $C/RT$ and $m^*/m$ near $T=0°K$ was obtained by drawing the best straight line between the data near 0.03°K and the origin. The results for various pressures are displayed on Fig. 2. There is no experimental justification for this procedure at the higher pressures. At zero pressure we find that $C/RT = 2.78\ (K°)^{-1} \pm 10\%$ and $m^*/m = 2.82 \pm 10\%$, using the formula

$$\frac{m^*}{m} = \frac{C}{RT}\frac{\hbar^2}{mk}\left(\frac{3}{\pi}\frac{N}{V}\right)^{2/3}, \tag{1}$$

where all symbols have their usual meaning.[1] At these temperatures $(C_p - C_v)/C_p$ is negligibly small. This value of $m^*/m$ is to be compared with the extrapolation from 0.085°K of reference 3 giving $m^*/m = 2.00 \pm 0.05$, and with the extrapolation from 0.054°K of reference 2 giving $m^*/m = 2.19 \pm 0.13$. These are consistent with the curve of $C/R$ vs $T$ bending in the region of 0.03-0.04°K, the same temperature above which the thermal conductivity began to deviate from the Fermi liquid temperature dependence.[17] The theoretical value of $m^*/m$ of Brueckner and Gammel[4] is 1.84. Summing the spin and nonspin contributions to the specific heat calculated by Goldstein,[5] we find $C/RT = 2.74\ (K°)^{-1}$, which corresponds to $m^*/m = 2.78$.

Below 25 atm, the limiting values of $C/RT$ are linear in $p$ and may be used to obtain the isobaric expansion coefficient. Using the formula, valid near $T=0°K$,

$$\frac{\partial \alpha_p}{\partial T} = -\frac{R}{V}\left[\frac{\partial}{\partial p}\left(\frac{C}{RT}\right)\right]_T, \tag{2}$$

where $\alpha_p = (1/V)(\partial v/\partial T)_p$ and $v$ is the molar volume, we find at zero pressure

$$-\partial \alpha_p/\partial T = 0.08\ (K°)^{-2}, \tag{3}$$

as a lower limit. Brueckner and Atkins[18] obtain 0.076 $(K°)^{-2}$ for this quantity, using results which gave the effective mass incorrectly. Goldstein[5] predicts 0.103 $(K°)^{-2}$. Brewer and Daunt[19] calculate from their data 0.105 $(K°)^{-2} \pm 25\%$. Recently, Rives and Meyer[20] found $\alpha_p = -(0.12 \pm 0.02)T$ between 0.04 and 0.08°K at 0.18 atm.

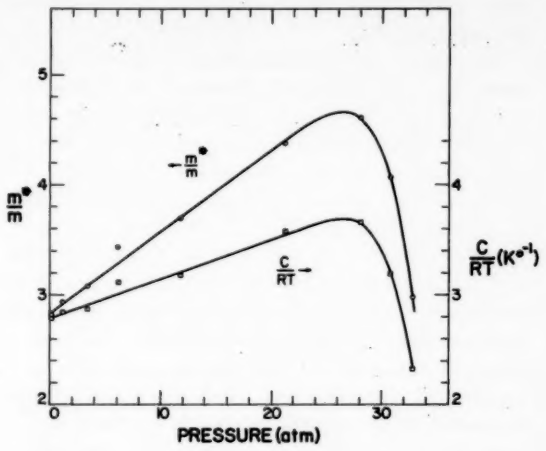


FIG. 2. Variation of lower limits of $m^*/m$ and $C/RT$ with pressure. The points on this graph were obtained by taking the slope of the best straight line through the data near 0.03°K and the origin. Below 25 atm, the slopes of the curves are $(d/dp)(m^*/m) = 0.074\ \text{atm}^{-1}$ and $(d/dp)(C/RT) = 0.036\ (\text{atm °K})^{-1}$.

We measured the specific heat and thermal boundary resistance of liquid $He^3$ at pressures above $P_{min}$ and at temperatures of 0.02°K and somewhat above by applying pressures of 30.7 and 32.8 atm near 1°K and then cooling through the solid and back into the liquid. In this region both the specific heat and the thermal boundary resistance are anomalously low, and the specific heat had the opposite pressure dependence from that at somewhat lower pressures. During measurements taken when a plug formed in the filling tube at a pressure of 32.8 atm, the specific heat became very high at temperatures higher than $0.030 \pm 0.001$°K, indicating the liquid-solid phase transition. For an external pressure of 34.8 atm, we found no evidence of two-phase equilibrium between 0.017°K and 0.036°K, and hence, we conclude that our specific heat measurements for these conditions were for the solid only. The results of Sydoriak, Mills, and Grilly[21] indicate that, if the molar volume in the cell were the same as that in the liquid just before solidification commenced, it would be impossible to have only solid $He^3$ in the cell. Hence, we conclude that during the formation of the plug in the capillary leading to the cell, additional $He^3$ enters the

cell. This effect can be observed in the external pressure system.

The results of specific heat measurements of solid $He^3$ for an external pressure of 34.8 atm are displayed on Fig. 1. Although the data are not precise enough to determine the temperature dependence of the specific heat, the specific heat does decrease as $T$ increases. The theory of Bernardes and Primakoff[8] predicts, for a body-centered cubic crystal, that $C/R = 3J^2/k^2T^2$, where $J/k$ is the exchange energy in temperature units. Assuming that the data fit a $1/T^2$ law, we find an average value for $|J/k|$ of 0.0015°K. This is about 10 times lower than the value of $J/k$ (= -0.02°K) calculated in reference 8 for a face-centered cubic crystal. Since in the neighborhood of the melting curve and at low temperatures the entropy of the solid is unexpectedly high and the entropy of the liquid is unexpectedly low, it is not surprising that the predicted[8,22] maximum in the melting pressure curve has not yet been observed. The rate of heat transfer between solid $He^3$ and the walls is comparable to that of the liquid and the walls.

The pressure of the minimum in the melting pressure curve was measured several times by observing the sudden increase in temperature of the CMN when the $He^3$ pressure decreased slowly through $P_{min}$, and the $He^3$ plug broke. We find $P_{min} = 29.0 \pm 0.1$ atm. This agrees, within experimental error, with $P_{min} = 28.91 \pm 0.02$ atm obtained by Sydoriak, Mills, and Grilly[21] and $P_{min} = 29.1 \pm 0.1$ atm obtained by Lee, Fairbank, and Walker.[15] It is slightly lower than the $P_{min} = 29.3 \pm 0.1$ atm obtained by Baum, Brewer, Daunt, and Edwards.[23]

We wish to acknowledge helpful discussions with Professor John Bardeen. We are grateful for the advice given us by Dr. H. A. Reich and D. Fitchen in the construction of the pressure system. Dr. R. F. Nyström very kindly measured the tritium contamination in the $He^3$. We wish to thank R. Sarwinski and W. Abel for help in the construction and running of the experiment, and J. Morr for assisting with the reduction of the data.

*This work was supported by the U. S. Atomic Energy Commission, the Alfred P. Sloan Foundation, and the Office of Naval Research. It is being submitted by G. L. Salinger in partial fulfillment of the requirements for the Ph.D. degree at the University of Illinois.

†National Science Foundation Fellow.

‡A. P. Sloan Fellow.

[1]A. C. Anderson, G. L. Salinger, W. A. Steyert, and J. C. Wheatley, Phys. Rev. Letters 6, 331 (1961).

[2]M. Strongin, G. O. Zimmerman, and H. A. Fairbank, Phys. Rev. Letters 6, 404 (1961).

[3]D. F. Brewer, J. G. Daunt, and A. K. Sreedhar, Phys. Rev. 115, 836 (1958).

[4]K. A. Brueckner and J. L. Gammel, Phys. Rev. 109, 1040 (1958).

[5]L. Goldstein, Phys. Rev. 117, 375 (1960).

[6]K. A. Brueckner, T. Soda, P. W. Anderson, and P. Morel, Phys. Rev. 118, 1442 (1960).

[7]V. J. Emery and A. M. Sessler, Phys. Rev. 119, 43 (1960).

[8]N. Bernardes and H. Primakoff, Phys. Rev. 119, 968 (1960).

[9]Furane Plastics, Inc., 4516 Brazil Street, Los Angeles 39, California.

[10]G. L. Salinger and J. C. Wheatley, Rev. Sci. Instr. 32, 872 (1961).

[11]Mansfield and Green, Inc., 1051 Power Avenue, Cleveland 14, Ohio.

[12]Helicoid Gauge Division, American Chain and Cable, Inc., Bridgeport 2, Connecticut.

[13]A. C. Anderson, G. L. Salinger, and J. C. Wheatley (to be published).

[14]R. H. Sherman and F. J. Edeskuty, Ann. Phys. 9, 522 (1960).

[15]D. M. Lee, H. A. Fairbank, and E. J. Walker, Phys. Rev. 121, 1258 (1961).

[16]Micro-Circuits Company, New Buffalo, Michigan.

[17]A. C. Anderson, G. L. Salinger, and J. C. Wheatley, Phys. Rev. Letters 6, 443 (1961).

[18]K. A. Brueckner and K. R. Atkins, Phys. Rev. Letters 1, 315 (1958).

[19]D. F. Brewer and J. G. Daunt, Phys. Rev. 115, 843 (1959).

[20]J. E. Rives and H. Meyer (private communication).

[21]S. G. Sydoriak, R. L. Mills, and E. R. Grilly, Phys. Rev. Letters 4, 495 (1960).

[22]N. Bernardes and H. Primakoff, Phys. Rev. Letters 2, 290 (1959); Phys. Rev. Letters 3, 144 (1959).

[23]J. L. Baum, D. F. Brewer, J. G. Daunt, and D. O. Edwards, Phys. Rev. Letters 3, 127 (1959).

# PROPAGATION OF SOUND IN $He^3$†

W. R. Abel, A. C. Anderson, and J. C. Wheatley*
Department of Physics, University of Illinois, Urbana, Illinois
(Received September 18, 1961)

We have studied the propagation of sound in $He^3$ over a range of pressures extending from 1.4 psi to 513 psi. At low pressures we have obtained the sound attenuation coefficient and have interpreted it in terms of a viscosity, the results being in satisfactory agreement with experiments on other transport properties in $He^3$. In a pressure region somewhat above the minimum, $P_{min}$, in the melting curve, we find a sharp break both in the velocity of propagation of sound and in the temperature dependence of the attenuation coefficient.

The experimental cryogenic apparatus is similar to others which have been described elsewhere.[1,2] The sound cell was sealed into a nonmagnetic epoxy resin bulb with a powder of cerium magnesium nitrate which served as the thermometer. The sound cell consisted of an "X"-cut quartz crystal of nominal frequency 5 Mc/sec separated from an optically flat fused quartz reflector by a fused quartz ring of thickness 0.1890 cm and bore 0.5 cm with parallel and optically flat faces. The ring had four radial grooves ground in one surface to allow entry of $He^3$. Measurements of velocity were made using standard ultrasonic pulse techniques, no fewer than two echoes being used for this purpose, although in some cases as many as fifteen echoes were used. The attenuation coefficient was obtained by fitting the echo heights, $h$, to the equation $h = h_0 e^{-\alpha x}$, where $\alpha$ is the attenuation coefficient and $x$ is the distance traversed by the sound.

At a pressure of 3.38 psi, measurements of the attenuation coefficient were made at frequencies of both 5.13 Mc/sec and 14.92 Mc/sec. Near 1°K the ratio of the apparent attenuation coefficients was nearly the ratio of the two frequencies, characteristic of geometric attenuation. However, below 0.1°K the ratio of the attenuation coefficients was, within experimental error, given by the ratio of the squares of the frequencies. This result is characteristic of viscous attenuation, for which the attenuation coefficient is given by[3]

$$\alpha = (8\pi^2\nu^2/3\rho c^3)\eta, \qquad (1)$$

where $\nu$ is the frequency, $\rho$ is the density, $c$ is the sound velocity, and $\eta$ is the viscosity. The experimental attenuation data are shown in Fig. 1. At 5.13 Mc/sec the geometrical attenuation coefficient is approximately 0.2 to 0.3 $cm^{-1}$. Below 0.05°K to 0.06°K the attenuation coefficient obeys a $T^{-2}$ law to within the accuracy of our measurements, the resulting viscosity being given by $\eta = 2.8\times10^{-6}T^{-2}$ dyne sec $(K°)^2/cm^2$. Using the result that $\eta = (\frac{1}{3}v_0^2\tau_\eta)\frac{3}{5}\rho(m^*/m)$, where $v_0$ is the Fermi velocity and $m^*/m$ is the ratio of quasiparticle mass to bare particle mass, to evaluate the relaxation time for viscosity, $\tau_\eta$, from the Fermi liquid theory,[3] we find $\tau_\eta = 17\times10^{-13}T^{-2}$

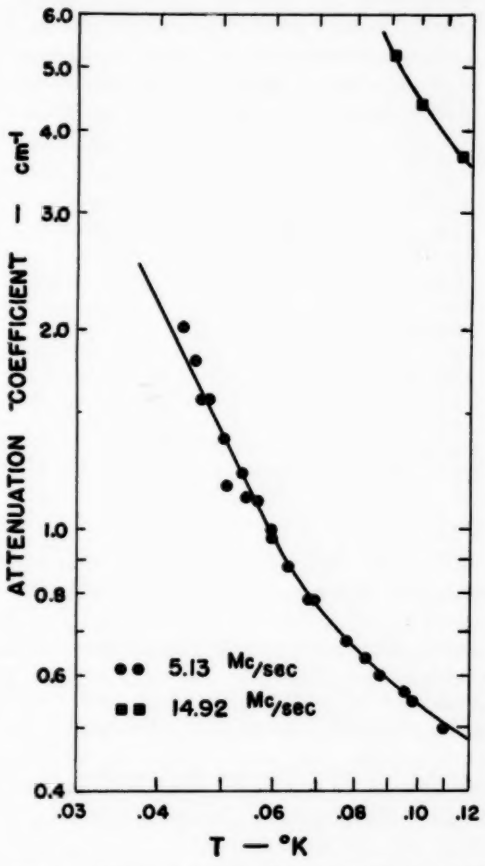


FIG. 1. Ultrasonic attenuation coefficient as a function of temperature in liquid $He^3$ at a pressure of 3.38 psi and at frequencies of 5.13 Mc/sec and 14.92 Mc/sec. The line through the experimental data at 5.13 Mc/sec for temperatures less than 0.06°K arbitrarily has been drawn with the $T^{-2}$ temperature dependence predicted by the Fermi liquid theory.[3]

Table I. Velocity of sound in liquid $He^3$ at various pressures and, for pressures less than 426 psi, for $T$ less than 0.1°K.

| Pressure (psi) | Velocity (m/sec) | Frequency (Mc/sec) |
|---|---|---|
| 1.42 | 184.0 | 5.13 |
| 8.06 | 192.1 | 5.13 |
| 13.97 | 198.5 | 5.13 |
| 16.25 | 201.0 | 5.13 |
| 50.8 | 231.2 | 5.13 |
| 89.9 | 260.2 | 5.13 |
| 174.3 | 306.8 | 14.92 |
| 314.6 | 361.8 | 14.92 |
| 414.1 | 394.2 | 14.92 |
| 423.9 | 396.8 | 14.92 |
| 425.9 | 397.9 | 14.92 |
| 433.6[a] | 397.9 | 14.92 |
| 483.2[a] | 408.6 | 14.92 |
| 513.0[a] | 416.9 | 14.92 |

[a]The velocities at these pressures were obtained with $T \simeq 1$°K.

sec $(K°)^2$. This relaxation time is 2.7 times that found for the thermal conductivity.[4] Using the values of $c$, $\rho$,[5] and[6] $m^*/m$ to compute $\tau_\eta/\tau_k$ from the Fermi liquid theory, we find the theoretical estimate to be $\tau_\eta/\tau_k = 1.5$.

At both 25 Mc/sec and 15 Mc/sec, sound measurements were attempted under excellent conditions at 0.008°K, but no echoes were observed.

The velocity of sound in liquid $He^3$ at various pressures less than $P_{min}$ and at temperatures of 0.1°K and below is given in Table I. We estimate an error of ±0.1% in the pressures and ±0.3% in the velocities. The extrapolated velocity at zero pressure is 182.4 ± 0.6 m/sec, which is to be compared with 183.9 ± 0.3 m/sec given by Laquer, Sydoriak, and Roberts.[7] Also given in Table I are velocities in the liquid near 1°K for a few pressures greater than $P_{min}$. These probably may be compared meaningfully with those below 0.1°K, for we found that at 424 psi the velocity did not change, within experimental error, between 1°K and 0.1°K.

At pressures greater than $P_{min}$, a plug of solid $He^3$ forms above the cell so that subsequent measurements are made at constant volume. In what follows, the pressures referred to are those in the liquid just before the plug is formed, and the frequency of the sound is 14.9 Mc/sec. The most striking features of the measurements in this region are assembled in Table II. For pressures of 435 psi and below, we found velocities at low temperatures which were a few percent larger than those observed for pressures just less than $P_{min}$. Moreover, the attenuation coefficient had both a magnitude and temperature dependence characteristic of the liquid at somewhat lower pressures. As the temperature increased, echoes were observed until the melting curve was reached, at which point we usually observed "double echoes" corresponding to propagation of sound between transmitter and reflector at both liquid and solid velocities, the latter being about 475 ± 10 m/sec. Eventually, only the solid velocity was observed, followed by more "double echoes" and then the velocity in the high-temperature liquid.

At pressures greater than 439 psi, the behavior of the liquid is remarkably different. At very low temperatures the sound velocity exceeds 500 m/sec, and hence is greater than the velocity in the solid. This effect was demonstrated strikingly at a pressure of 483 psi (not listed in Table II) where we observed a "double-echo" pattern characteristic of two-phase equilibrium and corresponding to a velocity ratio of 14:13 ≅ (510 m/sec:475 m/sec) in which the relative size of the high-velocity component steadily increased as the temperature decreased from 0.035°K to 0.016°K. In addition to having a sound velocity about 25% greater than that in the liquid at somewhat lower pressures, the $He^3$ in the high-pressure region is characterized by an attenuation which increases, rather

Table II. Characteristic sound parameters in $He^3$ at low temperatures and at pressures greater than the minimum in the melting curve.

| Pressure[a] (psi) | Velocity[b] (m/sec) | Temperature (°K) | Attenuation coefficient ($cm^{-1}$) |
|---|---|---|---|
| 431 | 409 | 0.030 | 0.9 |
| 431 | 405 | 0.1 | 0.5 |
| 431 | 402 | Melting curve | ... |
| 435 | 407 | 0.026 | 1.3 |
| 435 | 404 | 0.1 | 0.5 |
| 435 | 396 | Melting curve | ... |
| 439 | 503 | 0.030 | 1.0 |
| 439 | 485 | 0.1 | 1.6 |
| 454 | 510 | 0.022 | 1.1 |
| 454 | 491 | 0.1 | 2.8 |

[a]These are the pressures at which the capillary plugged.

[b]Accuracy of velocity measurements is about 1%.

than decreases, with increasing temperature. Above the temperature region near 0.1°K we were unable to make measurements because of the high attenuation. Hence, as we increased the temperature above 0.1°K we saw practically no echoes until suddenly large echoes characteristic of the solid became visible, corresponding to the transition back into the solid.

At a pressure of 513 psi we observed echoes in the solid only, the velocity being constant within experimental error from 1°K to 0.017°K. According to the work of Sydoriak, Mills, and Grilly,[8] if the molar volume of the $He^3$ in the cell after the plug was formed remained constant at that for the liquid just before the plug formed, it would be impossible to have only solid $He^3$ in the cell for any of the pressures for which we made measurements. At an external pressure of 513 psi, and possibly at lower pressures also, we observed echo patterns characteristic of the solid only. Hence, we conclude that during the process of forming a plug in the tube leading to the cell, a substantial amount of $He^3$ passes into the cell. This conclusion is supported by work reported in reference 6, where under similar conditions the heat capacity characteristic of the solid only was observed.

In the above measurements the pressure of the $He^3$ below the plug was not known and probably varied with temperature. Moreover, above 0.1°K the large attenuation made sound measurements impossible. However, the measurements do indicate that below 0.1°K and in a narrow pressure region near 437 psi there is a drastic change in both the velocity and attenuation of sound. Moreover, it has been observed recently[6] that in this same region the specific heat is considerably lower and has the opposite pressure dependence from that in the liquid at pressures just less than $P_{min}$. Hence, it appears likely that in this high-pressure region we are dealing with a different phase of $He^3$ from that which occurs at lower pressures.

We are indebted to Professor John Bardeen for helpful discussions. We wish gratefully to acknowledge the assistance of E. N. Koch, M. Kuchnir, W. Reese, G. L. Salinger, and R. J. Sarwinski, who aided us in assembling and running the experiments and in treating the experimental data.

---

†This work was supported by the U. S. Atomic Energy Commission and by the Alfred P. Sloan Foundation.

*A. P. Sloan Fellow.

[1]A. C. Anderson, G. L. Salinger, W. A. Steyert, and J. C. Wheatley, Phys. Rev. Letters 6, 331 (1961).

[2]A. C. Anderson, G. L. Salinger, and J. C. Wheatley, Rev. Sci. Instr. (to be published).

[3]A. A. Abrikosov and I. M. Khalatnikov, Reports on Progress in Physics (The Physical Society, London, 1959), Vol. 32, p. 329.

[4]A. C. Anderson, G. L. Salinger, and J. C. Wheatley, Phys. Rev. Letters 6, 443 (1961).

[5]R. H. Sherman and F. J. Edeskuty, Ann. Phys. 9, 522 (1960).

[6]A. C. Anderson, G. L. Salinger, W. A. Steyert, and J. C. Wheatley, preceding Letter [Phys. Rev. Letters 7, 295 (1961)]. $m^*/m = 2.82$.

[7]H. L. Laquer, S. G. Sydoriak, and T. R. Roberts, Phys. Rev. 113, 417 (1959).

[8]S. G. Sydoriak, R. L. Mills, and E. R. Grilly, Phys. Rev. Letters 4, 495 (1960).

# SUPERCONDUCTIVITY OF NIOBIUM-MOLYBDENUM ALLOYS BELOW 1°K

J. K. Hulm and R. D. Blaugher
Westinghouse Research Laboratories, Pittsburgh, Pennsylvania

and

T. H. Geballe and B. T. Matthias
Bell Telephone Laboratories, Murray Hill, New Jersey

(Received September 18, 1961)

The alloys between group 5 and group 6 transition elements are of great interest due to the availability of a continuous range of solid solution between superconductor and nonsuperconductor.[1] In previous work the systems V-Cr, Nb-Mo, Ta-W, and Nb-W were studied down to 1°K and it was observed that the transition temperature of the superconducting component was lowered by the addition of the nonsuperconductor. The depression of $T_c$ was found to be roughly proportional to concentration.

It is of interest to know whether the observed linear relationship between $T_c$ and composition extends below 1°K, particularly since such a relationship appears to be in conflict with the prediction of the Bardeen-Cooper-Schrieffer (BCS) theory.[2] The theory, with some simplifying assumptions,[3] gives

$$T_c = 0.855\,\theta \exp[-1/N(0)V], \qquad (1)$$

where $\theta$ is the Debye temperature, $N(0)$ is the density of states at the Fermi surface, and $V$ is the (positive) interaction potential giving rise to the superconducting state.

The niobium-molybdenum system was chosen for detailed study below 1°K. A number of compositions in the range 35 to 45 atomic percent molybdenum were prepared by levitation melting followed by high-temperature annealing (2500°C). The composition and impurity content were determined by chemical, gaseous, and spectroscopic methods. Superconducting transition temperatures below 1°K were determined in a helium-3 cryostat using an ac method.[4] Sharp superconducting transitions were obtained after improving the metallurgical techniques. Transition breadths ranging from 0.01°K up to 0.1°K were found for most samples. The resulting data are shown in Fig. 1 with the region below 1°K shown in detail in the insert.

The dashed curve in Fig. 1 is calculated from Eq. (1) using $N(0)$ and $\theta$ values interpolated linearly between the known values for pure niobium and pure molybdenum and assuming the value of $V$ for niobium remains constant.[5] While such a procedure is arbitrary, the long exponential approach to absolute zero is characteristic of the theory, not the procedure. The present experiments show an almost linear dependence of $T_c$ which extrapolates to zero at a finite composition, in conflict with the above application of the simplified theory. The possibility of this difference between theory and experiment has been emphasized by Pippard.[6] It is further illustrated in Fig. 2 where we replot the same data as Fig. 1 in the coordinate scheme suggested by Eq. (1). In this case the BCS plot is practically linear whereas the very steep descent of the experimental curve is well brought out.

The linearly interpolated values of $N(0)$ and $\theta$ require that $V$ in Eq. (1), or more precisely $N(0)V/\gamma$ where $\gamma$ is the electronic specific heat coefficient, be the parabolic function of concentration shown in Fig. 1. A more rapidly varying $N(0)$ than assumed would rotate the $V$ curve counterclockwise about the point for pure Nb and thus lessen the rapid descent of $V$ near 60% Nb. However, as the extrapolation in Fig. 1 indicates, $T_c$ almost certainly goes to zero at an intermediate concentration,[7] and therefore $V$ must go to zero. Any deviation of the true $N(0)$ from linearity should be due to the minimum in the density of states as Mo is approached and therefore would increase the curvature of the $V$ curve as it approaches zero. It might be expected that a rapid change in $V$ would be reflected in other ways; however, the known physical properties of the Nb-Mo system show no drastic changes in the pertinent concentration region. Since $V$ is the difference between the attractive phonon and repulsive Coulomb potentials, it possibly is a delicate function whose variation is not manifested in other ways. However, the mere fact that a large variation of $V$ has to be assumed is contrary to the fact that $T_c$ is a simple function of $N(0)$ alone throughout the periodic system.[8] Such can be the case only if $V$ is essentially constant, as indeed was assumed by Pines[5] in explaining the periodic occurrence of superconductivity in the transition elements, or is a simple function of $N(0)$ itself. We are left with the dilemma

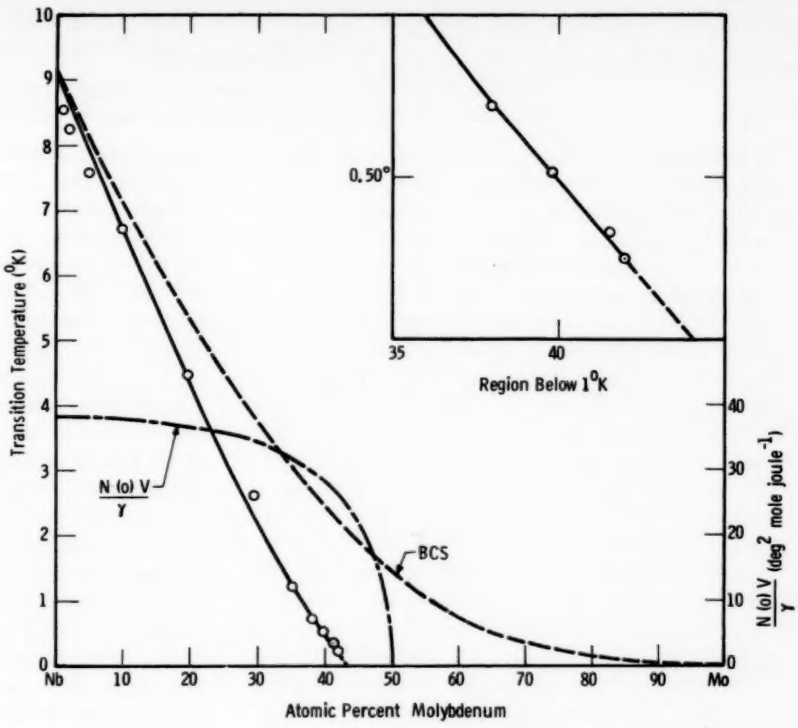


FIG. 1. Variation of the superconductivity transition temperature with composition in the Nb-Mo system. The dashed BCS curve shows the transition temperature calculated from Eq. (1) using a constant $V$. The $N(0)V/\gamma$ curve shows the variation in $V$ which must be assumed to make Eq. (1) give the measured (and extrapolated) curve.

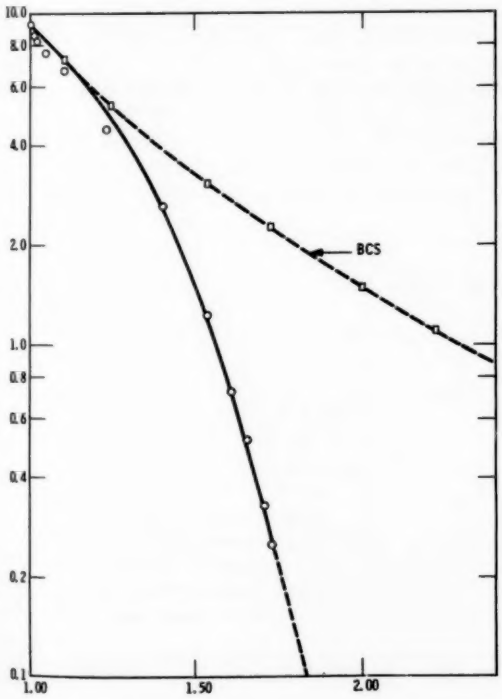


Fig. 2. Same data as Fig. 1 using semilog coordinates.

that such a $V$ is not consistent with the present data.

We would like to thank G. Comenetz for his levitation melting of the samples, G. W. Hull for help with the measurements, and P. Nozières, J. C. Phillips, and P. Morel for their helpful comments.

[1]J. K. Hulm and R. D. Blaugher, Phys. Rev. 123, 1569 (1961).

[2]J. Bardeen, L. N. Cooper, and J. R. Schrieffer, Phys. Rev. 108, 1175 (1957).

[3]B. V. Goodman, J. Hillarret, J. J. Veyssie, and L. Weil, Proceedings of the Seventh International Conference on Low-Temperature Physics, 1960 (University of Toronto Press, Toronto, 1960), p. 350.

[4]T. H. Geballe, B. T. Matthias, G. W. Hull, Jr., and E. Corenzwit, Phys. Rev. Letters 6, 275 (1961).

[5]D. Pines, Phys. Rev. 109, 280 (1958).

[6]A. B. Pippard, remarks at the IBM Conference on Superconductivity, June, 1961 (unpublished).

[7]This is also true when Mo-Re alloys are considered as shown in Fig. 8 of reference 1.

[8]J. G. Daunt, Progress in Low-Temperature Physics (North-Holland Publishing Company, Amsterdam, 1955), Vol. I; B. T. Matthias, ibid., Vol. II, 1957; H. W. Lewis, Phys. Rev. 101, 939 (1956); C. Kittel, Introduction to Solid State Physics (John Wiley & Sons, Inc., New York, 1956), 2nd ed., Fig. 16.2(b); and R. D. Blaugher and J. K. Hulm, J. Phys. Chem. Solids 19, 134 (1961).

# PARAELASTICITY, A MECHANICAL ANALOG OF PARAMAGNETISM

Werner Känzig*
General Electric Research Laboratory, Schenectady, New York
(Received June 30, 1961; revised manuscript received September 1, 1961)

It is known that certain radicals imbedded in a solid matrix of high symmetry can rotate even at very low temperatures.[1] An interesting question to ask is: Is it possible to limit this rotation, i.e., to "align" the radicals, by a mechanical stress applied to the host crystal? For imperfections that interact rather strongly with the matrix it has been shown by various techniques (internal friction,[2] electron spin resonance[3]) that alignment can be achieved. However, the stress-alignable systems that have been reported so far freeze in at relatively high temperatures, and the kinetics of the hindered rotation is given by the conventional thermal activation theory (Arrhenius plot).

In the present paper we report on a radical in alkali halides that has a different kinetic behavior. It still "rotates" at very low temperatures, and yet it can be aligned by modest mechanical stresses. It is the $O_2^-$ radical, which substitutes for a halide ion. A paramagnetic resonance study has shown that the internuclear axis of the $O_2^-$ molecule ions has six equilibrium orientations, namely, along the [110] axes of the crystal.[4] In the unstressed crystal all six orientations are equally probable. If a mechanical stress is applied, the equilibrium orientations still correspond to [110] axes; however, the six [110] axes are no longer equally populated.

This system lends itself very well to an accurate measurement of the orientational distribution by means of paramagnetic resonance for the following reasons: (1) The anisotropy of the $g$ factor is sufficiently large so that the paramagnetic resonance spectra corresponding to the six equilibrium orientations can be separated. (2) The $O_2^-$ molecule ion is very little affected by the stress field (except for its orientation). Therefore, the intensity of the paramagnetic resonance arising from the molecule ions oriented along a given [110] axis is a direct measure of their number. Thus we measured the stress alignment as a function of compressional uniaxial stress along [111], [110], and [100], and as a function of temperature in the range from 1.5°K to 33°K for the host crystals KCl, KBr, and KI.

For static stresses the distribution of the $O_2^-$ radicals over the orientations, that become nonequivalent through the stress, was found to obey Boltzmann statistics. The energy differences occurring in the Boltzmann factors are proportional to the stress $X$. Figure 1 serves to illustrate these

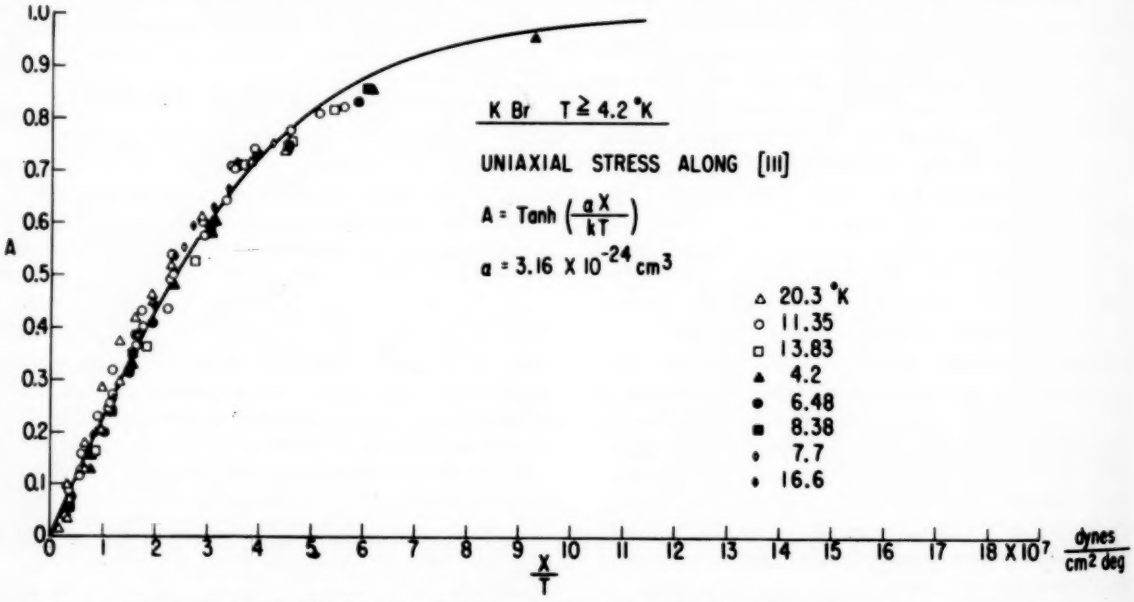


FIG. 1. Alignment $A=(N_1-N_2)/(N_1+N_2)$ of $O_2^-$ molecule ions in KBr for uniaxial stress $X$ along [111], versus $X/T$. The solid curve is the calculated curve $\tanh(\alpha X/kT)$ for $\alpha=3.16\times10^{-24}$ cm$^3$.

Table I. Anisotropic part $\Delta r_{jj}'$ of the misfit, as determined from the experimental Boltzmann factors. Units $10^{-8}$ cm.

| | $\Delta r_{xx}'$ | $\Delta r_{yy}'$ | $\Delta r_{zz}'$ |
|---|---|---|---|
| KCl | -0.04 | -0.40 | +0.44 |
| KBr | -0.15 | -0.26 | +0.41 |
| KI | -0.32 | -0.19 | +0.51 |

facts for uniaxial stress along [111]. This stress gives rise to two energetically nonequivalent orientations, 1 and 2, so that the alignment $A=(N_1-N_2)/(N_1+N_2)$ is given by the well-known Brillouin function for two energy levels.

The interaction of the $O_2^-$ radical with the external stress was analyzed in terms of the continuum theory of lattice imperfections.[5] The $O_2^-$ radical was treated as an ellipsoidal inclusion in an elastic medium. The $z$ axis of the ellipsoid was chosen along the internuclear axis, and the $x$ axis along the lobes of the $p$ function of the unpaired electron.[4] If one assumes that the elastic constants of the inclusion are close to those of the matrix, one obtains for the energy change of the inclusion due to an external stress[6]

$$U \cong \tfrac{4}{3}\pi a^2(S_{xx}\Delta r_{xx}+S_{yy}\Delta r_{yy}+S_{zz}\Delta r_{zz}). \qquad (1)$$

Here $a$ is the radius of the site (halide ion), $S_{jj}$ is the component of the stress along the axis $j$ of the inclusion, and $\Delta r_{jj}$ is the difference between the radius of the free molecule ion along its axis $j$ and the radius $a$ of the halide ion. The experimental results are internally consistent with Eq. (1) and permit the determination of the anisotropic part $\Delta r_{jj}'$ of the misfit, $\Delta r_{jj}'=\Delta r_{jj}-\frac{1}{3}(\Delta r_{xx}+\Delta r_{yy}+\Delta r_{zz})$. The result is given in Table I. The numbers show that the molecule ion is cigar-shaped with the longest axis along $z$.

Table II. Constant $B$ of the relation $\tau=B/T$. Units sec degree.

| Stress axis | $B$ [111] | [110] | [100] |
|---|---|---|---|
| KCl | 21 ±3 | 9 ±3 | 11 ±3 |
| KBr | | | 4 ? |
| KI | 61 ±5 | 76 ±5 | 77 ±2 |

The kinetics of the alignment process can be studied by monitoring the intensity of paramagnetic resonance lines upon sudden application or removal of the stress, since the paramagnetic relaxation time $T_1$ is at least one order of magnitude shorter than the reorientation times.[7] The time $\tau^*$ for alignment decreases with increasing stress, whereas the time $\tau$ for recovery is independent of the magnitude of the stress, as is exemplified in Fig. 2. Below 4.2°K the time $\tau$, as well as $\tau^*$ for moderate stresses, is inversely proportional to the temperature $T$, i.e., $\tau=B/T$. Thus the system can be considered as a mechanical analog of paramagnetism, not only with regard to its static behavior (Fig. 1), but also with regard to its relaxation behavior at very low temperatures. The experimental values of $B$ are given in Table II.

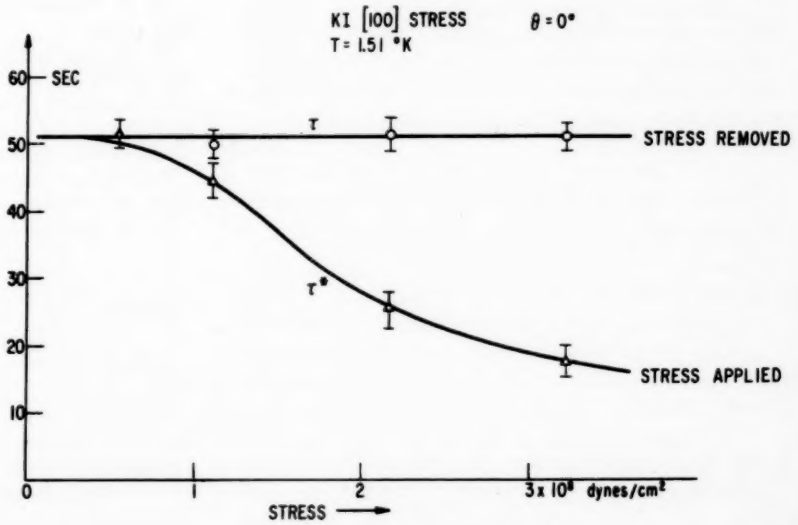


FIG. 2. Example for stress dependence of the alignment time $\tau^*$ and stress independence of the reorientation time $\tau$. KI stressed along [100] at 1.51°K.

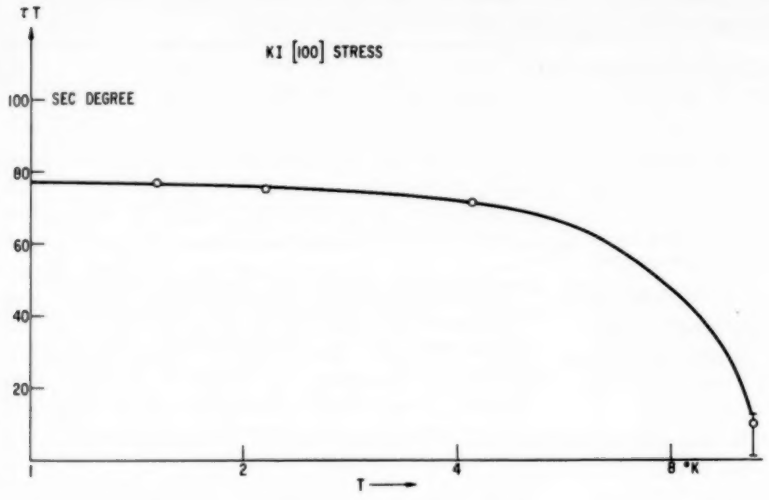


FIG. 3. Example of temperature dependence of the product $\tau T$. KI stressed along [100].

The anisotropy of the reorientation kinetics is (within experimental error) consistent with the assumption that the reorientation involves two basic processes, namely, a 90° rotation in a (100) plane with the probability $p_1$, and a 60° rotation out of a (100) plane with the probability $p_2$. The analysis of the rate equations, using the $B$ values in Table II, yields:

for KCl, $p_1 \ll p_2$,

$$p_2/T = (15 \pm 3) \times 10^{-3} \text{ sec}^{-1} \text{ degree}^{-1},$$

for KI, $p_1/T = (3.8 \pm 0.4) \times 10^{-3} \text{ sec}^{-1} \text{ degree}^{-1}$,

$$p_2/T = (2.2 \pm 0.2) \times 10^{-3} \text{ sec}^{-1} \text{ degree}^{-1}.$$

The $B/T$ law suggests that the reorientation of the $O_2^-$ radical involves emission or absorption of one phonon. If this is true, the ultrasonic absorption versus stress should exhibit resonance peaks ("paraelastic resonance"). Inverted populations can be generated by reversing the stress so that mechanically pumped phonon masers might become feasible.

Above 4.2°K the time $\tau$ becomes much shorter than $B/T$ (Fig. 3). Usual thermal activation seems to take over.

A detailed account of the present investigations will be published elsewhere. The author gratefully acknowledges the cooperation of G. D. Watkins, W. G. Johnston, T. G. Castner, and G. E. Nichols. Special thanks are due to M. H. Cohen for active help at important stages of the interpretation.

---

*Present address: Physikalisches Institut E. T. H., Zürich, Switzerland.

[1]C. K. Jen, in Formation and Trapping of Free Radicals, edited by A. M. Bass and H. P. Broida (Academic Press, Inc., New York, 1960), pp. 235-238.

[2]A. S. Nowick, in Progress in Metal Physics, edited by B. Chalmers (Interscience Publishers, Inc., New York, 1953), Vol. 4, p. 30.

[3]G. D. Watkins and J. W. Corbett, Phys. Rev. 121, 1001 (1961).

[4]W. Känzig and M. H. Cohen, Phys. Rev. Letters 3, 509 (1959).

[5]J. D. Eshelby, in Solid-State Physics, edited by F. Seitz and D. Turnbull (Academic Press, Inc., New York, 1956), Vol. 3, pp. 95-99.

[6]The author owes the explicit derivation of this formula to M. H. Cohen.

[7]T. G. Castner (private communication).

# DOUBLE RESONANCE AND NUCLEAR COOLING IN AN ANTIFERROMAGNET*

A. J. Heeger,† A. M. Portis,‡ Dale T. Teaney,‖ and Gerald Witt†
Department of Physics, University of California, Berkeley, California
(Received September 18, 1961)

We wish to report the observation of the $Mn^{55}$ nuclear resonance by a double-resonance technique in the antiferromagnet $KMnF_3$. In addition, by observing the nuclear spin temperature as a function of power absorbed by the electronic antiferromagnetic resonance, we have discovered an apparent cooling of the nuclei via their interactions with the electron system.

Examination of the antiferromagnetic resonance of $KMnF_3$ in the liquid helium temperature range shows that even at these low temperatures there is a strong temperature dependence of the resonance field as is shown for one of the absorption lines by the experimental points of Fig. 1. We have interpreted this shift to be the result of a strongly temperature-dependent anisotropy field arising from the hyperfine interaction of the antiferromagnetic system with the $Mn^{55}$ nuclear moments. This hyperfine anisotropy field has the form

$$H_{A_1} = (A/g\mu_B)\langle I_z \rangle.$$

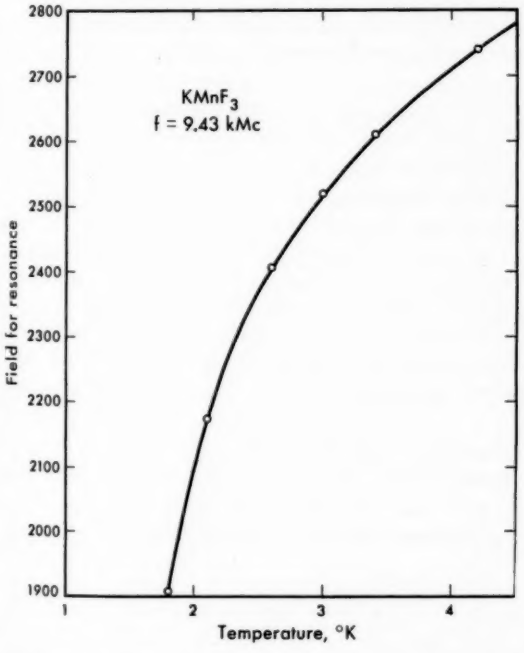


FIG. 1. Theoretical fit of the temperature dependence of the resonance field. The mechanism is the temperature dependence of the hyperfine anisotropy field.

The hyperfine constant $A/g\mu_B$ has been evaluated experimentally by Ogawa[1] from the paramagnetic resonance of $Mn^{2+}$ in isomorphous compounds. Substituting Ogawa's value of 92 oe, we obtain

$$H_{A_1} = 8.0/T \text{ oe}.$$

The expression for the resonance field of the electronic antiferromagnetic resonance is

$$H_0 = -\tfrac{5}{2}H_{A_2} + [\tfrac{9}{4}H_{A_2}^2 + (\omega/\gamma)^2 + 5H_E H_{A_4} - 2H_E H_{A_1}]^{1/2}.$$

The anisotropy field $H_{A_2}$ is responsible for the canting in this material[2] and is equal to 1300 oe as determined from measurements of the magnitude of the weak moment. The field $H_{A_4}$, which is associated with the cubic and axial anisotropy,[3] and the exchange field, $H_E$, were determined as 3.6 oe and $1.6\times10^6$ oe, respectively, by fitting theory and experiment. From the above expression it may be seen that the shift in resonance field resulting from the nuclear magnetization is of the order of $(H_E/H_0)H_{A_1}$. Thus a one-oersted nuclear field may produce a shift in resonance field by nearly one kilo-oersted. The completely satisfactory agreement between the experimental observations and this theory is shown in Fig. 1.

The strong dependence of the antiferromagnetic resonance field on nuclear spin temperature suggested the possibility of observing the $Mn^{55}$ nuclear resonance in antiferromagnetic $KMnF_3$ by a double-resonance technique. If enough rf power is supplied at the nuclear resonance frequency to saturate the nuclear magnetization, a shift of the antiferromagnetic resonance to its high-temperature position is expected. From the measurements of Ogawa the expected nuclear resonance frequency is

$$\nu_0 = (A/h)\langle S \rangle = 630 \text{ Mc/sec}.$$

The sample was a small cube of $KMnF_3$, approximately 1 mm on a side, at the center of a small rf coil, slightly over 1 mm in diameter. The sample and coil were placed at the bottom of a rectangular microwave cavity resonating in a $TE_{101}$ mode. A shift in the position of the antiferromagnetic resonance with rf power could be observed over a 42-Mc/sec range in frequency centered around 628 Mc/sec, in good agreement with the expected central frequency. In Fig. 2 is shown a

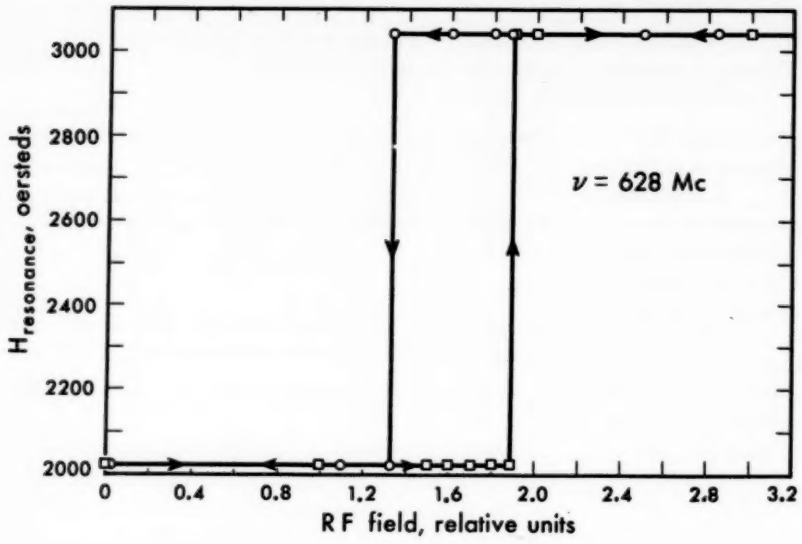


FIG. 2. Location of the antiferromagnetic resonance at 2.0°K as a function of rf field at 628 Mc/sec. The shift arises from the saturation of the nuclear magnetization.

plot of the location of the antiferromagnetic resonance as a function of rf field at the central frequency. It is found that when the rf field exceeds a critical value the electronic resonance line shifts abruptly to a new position characteristic of a high nuclear temperature. On reducing the rf field we find that the resonance line remains at its high-field position down to rf power levels well below those required for the initial shift.

By pulsing the 628-Mc/sec rf field on and then off, it was possible to observe the recovery of the position of the antiferromagnetic resonance line after removing the rf power. Such a recovery curve after nuclear saturation at 2.1°K is shown in Fig. 3. The relaxation appears to be nearly exponential with a characteristic relaxation time of 50 msec.

The very large shifts indicate that the nuclear magnetization is nearly reduced to zero at the rf levels employed. We estimate the interaction of the $Mn^{55}$ nuclei via spin waves[4] to yield a characteristic time $T_2$ of the order of 0.15 $\mu$sec. With the observed $T_1$ of about 50 msec, the rf field for partial saturation should be approximately 2 oe. This is actually about the level at which the nuclear saturation jumps to nearly its full value. As is shown in Fig. 2 the nuclear saturation may actually be maintained at rf fields well below this value. We have analyzed the excitation of the $Mn^{55}$ nuclei in some detail in an effort to understand the complex behavior observed. We find that because of the large parallel susceptibility of a canted antiferromagnet,[5] the $Mn^{55}$ nuclear resonance is excited indirectly by the sublattice magnetization rather than directly by the rf field. However, the $Mn^{55}$ nuclei themselves very strongly inhibit the sublattice excitation in the vicinity of the nuclear resonance as long as there is a substantial nuclear moment. This theory indicates that it should be harder to produce an initial saturation of the nuclei against their dynamical resistance than to maintain the saturation when there is very little

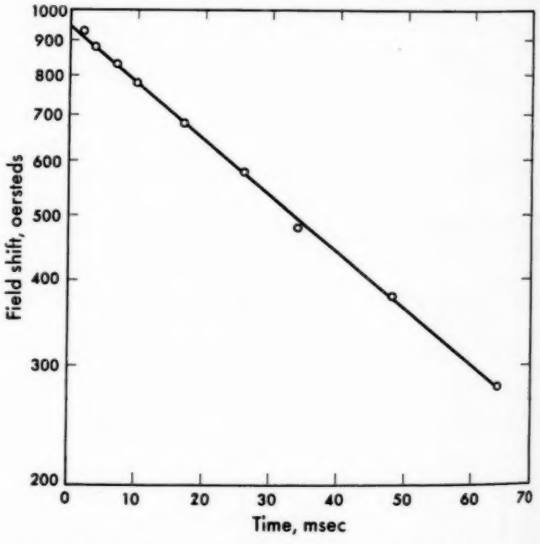


FIG. 3. Recovery curve showing the shift of the antiferromagnetic resonance at a given time after turning off the 628-Mc/sec rf power.

nuclear moment, in agreement with the observed hysteresis shown in Fig. 2. The frequency range over which such behavior may be expected depends on the nuclear magnetization and bears very little relation to the actual linewidth $1/T_2$.

Experiments have also been performed[6] in which the antiferromagnetic resonance is driven at high microwave levels without any direct nuclear excitation. Under these conditions we also find a shift in the position of the antiferromagnetic resonance. This shift is clearly associated with a change in nuclear magnetization. The apparent nuclear temperature as a function of microwave power for several lattice temperatures is shown in Fig. 4. At 4.2°K the nuclear temperature remains constant up to the power at which spin-wave breakdown occurs.[6] At high power levels the increased nuclear temperature presumably reflects the general increase in the level of excitation of the magnetic system. At 2.1 and 1.8°K there is a quite unexpected reduction in the nuclear temperature before the onset of spin-wave heating. At these lower temperatures and low power levels the nuclei are evidently cooled through their interactions with the off-equilibrium spin-wave system. The cooling of nuclear spins may be related to the possible development of an Overhauser effect in ordered magnetic materials as discussed by Oguchi and Keffer.[7] It should be emphasized that although the present experiments are unusually sensitive to a change in nuclear temperature, they are not especially sensitive to the development of a uniform nuclear polarization. Such a polarization would shift the resonance in the same way as an external field. Full nuclear polarization would produce a shift of only a few oersteds and would be completely dominated by the shift resulting from even a slight change in nuclear temperature. The recovery of the position of the antiferromagnetic resonance following microwave saturation has been studied. The relaxation appears to be the same as that observed following direct rf saturation of the nuclei.

We wish to acknowledge the helpful comments of Professor T. Nagamiya and the hospitality of his laboratory extended to one of us (A.M.P.). The authors also benefited from several discussions with Dr. P. Pincus.

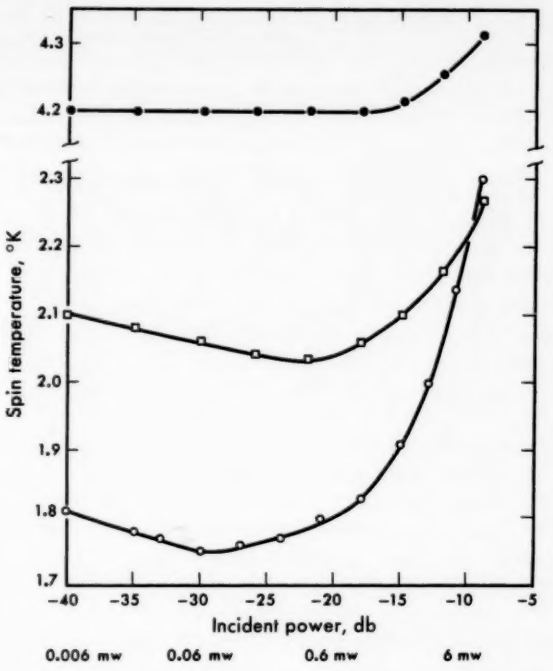


FIG. 4. Spin temperature as a function of microwave power absorbed by the sample. The spin temperature is determined by the resonance field.

---

*Work supported by the U. S. Atomic Energy Commission.

†National Science Foundation Cooperative Fellows.

‡Fulbright Research Scholar at Osaka University, 1961-62.

‖Present address: United Kingdom Atomic Energy Authority, Harwell, England.

[1]S. Ogawa, J. Phys. Soc. (Japan) 14, 1115 (1959).

[2]A. J. Heeger, Olof Beckman, and A. M. Portis, Phys. Rev. 123, 1652 (1961).

[3]J. J. Pearson, Phys. Rev. 121, 695 (1961).

[4]H. Suhl, Phys. Rev. 109, 606 (1958); T. Nakamura, Progr. Theoret. Phys. (Kyoto) 20, 542 (1958).

[5]R. Ohrbach, Phys. Rev. 115, 1189 (1959).

[6]A. J. Heeger, thesis, University of California, Berkeley, 1961 (unpublished).

[7]T. Oguchi and F. Keffer, Bull. Am. Phys. Soc. 3, 193 (1958).

# OBSERVATION OF THE MAGNETICALLY INDUCED MAGNETOELECTRIC EFFECT AND EVIDENCE FOR ANTIFERROMAGNETIC DOMAINS

G. T. Rado and V. J. Folen
U. S. Naval Research Laboratory, Washington, D. C.
(Received September 27, 1961)

In this Letter we report the first observation of the magnetically induced magnetoelectric effect [henceforth denoted by $(ME)_H$] in an antiferromagnetic material. When correlated with the previously observed[1,2] electrically induced magnetoelectric effect [henceforth denoted by $(ME)_E$], this observation provides a necessary verification of the existence of $EH$-type terms[3,4] in the thermodynamic potential of a spin-ordered substance. We also report the discovery of magnetic annealing effects in an antiferromagnet. In conjunction with other structure-sensitive phenomena which we found by means of magnetoelectric (ME) measurements, these magnetic annealing effects will be shown to provide the first strong evidence for the existence of antiferromagnetic "domains." Previous work[5] on such "domains" was largely speculative.

The thermodynamically derived[4] constitutive relations appropriate for the $(ME)_H$ effect are

$$D_z = \epsilon_{\parallel} E_z + \alpha_{\parallel} H_z, \quad D_{x,y} = \epsilon_{\perp} E_{x,y} + \alpha_{\perp} H_{x,y}, \tag{1}$$

where $\alpha_{\parallel}/4\pi$ and $\alpha_{\perp}/4\pi$ are magnetoelectric susceptibilities and the $z$ axis is chosen to be along the principal axis ($c$ axis) of a uniaxial crystal. In our experiments on $Cr_2O_3$ the applied electric field was zero. Using x-ray-oriented single-crystal disks whose cylindrical axes $z'$ were at an angle $\theta$ ($\theta = 0$, $90°$, and $\theta_1 \approx 30°$) to the $z$ axis, we switched on a magnetic field $H$ along $z'$ and measured the voltage $V$ which was induced between the silvered plane surfaces of the disks. For fields up to the highest values used ($H \approx 2500$ oe), $V$ was found to be proportional to $H$. Although $V$ decays with a relaxation time $\tau$ determined by the conductivity and dielectric constant of $Cr_2O_3$, the value of $\tau$ was found to be sufficiently large to permit us to measure $V$ with a vacuum tube electrometer (Keithley Instruments, Inc., Model 610R). In the vicinity of room temperature the low-voltage measurements could not be made because of drift in the apparatus. The actual voltage $V$ may not be equal to the open-circuit voltage $V^0$ (because the resistance of the disks may not be small in comparison to the input impedance of the electrometer), but it is clear the $V$ must be proportional to $V^0$ and hence [because of Eq. (1)] proportional to $\alpha$.

Our experimental results show that the temperature dependence of $V_{\parallel}$ and $V_{\perp}$ is essentially the same as that of the $\alpha_{\parallel}$ and $\alpha_{\perp}$ which we deduced from our $(ME)_E$ effect[2] experiments and described satisfactorily in a recent theoretical[6] study. As shown in Fig. 1, the temperature dependence of $|V_{\theta_1}|$ and $|\alpha_{\theta_1}{}^{app}|$ [which were measured by means of the $(ME)_H$ and $(ME)_E$ effects, respectively] are also in agreement. Since the values of antiferromagnetic permeabilities are close to unity, we find that $\alpha_\theta{}^{app}$ (the measured value of $\alpha_\theta$) is given by the relation $\alpha_\theta{}^{app} \approx [1 - (N_{z'}/4\pi)]\alpha_\theta$, where $N_{z'}$ is the axial demagnetizing factor of an oblate spheroid having the same axial ratio as the disks used in the ME measurements. Furthermore, we observed that the signs of $V_{\theta_1}$ and $\alpha_{\theta_1}{}^{app}$ reverse at the same temperature. We also found that the three ratios $|V_{\parallel}|/|\alpha_{\parallel}{}^{app}|$,

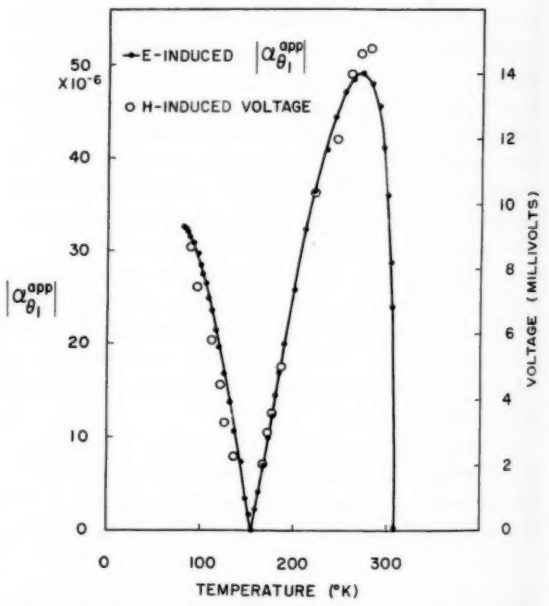


FIG. 1. Comparison of the temperature dependence of $|\alpha_{\theta_1}{}^{app}|$ and the induced voltage ($|V_{\theta_1}|$). These quantities were measured by means of the $(ME)_E$ and $(ME)_H$ effects, respectively. Both $\alpha_{\theta_1}{}^{app}$ and $V_{\theta_1}$ change sign near 154°K. The angle $\theta_1$ is about 30°.

$|V_\perp|/|\alpha_\perp{}^{app}|$, and $|V_{\theta_1}|/|\alpha_{\theta_1}{}^{app}|$ are equal to each other provided the $V$ and $\alpha^{app}$ contained in a given ratio are measured on the same sample.

Using both the $(ME)_H$ and the $(ME)_E$ effects, we observed that the signs and magnitudes of $\alpha_\parallel$ and $\alpha_\perp$, but not their temperature dependence, may vary (a) from sample to sample, and (b) upon cooling a sample through the Néel temperature either with or without the presence of a magnetic field. In view of (a), it is understandable that the relation $\alpha_\theta = \alpha_\parallel \cos^2\theta + \alpha_\perp \sin^2\theta$ (which follows from the form of the $\alpha$ tensor of $Cr_2O_3$) is not obeyed if the $\alpha$'s are measured on different samples. The magnetic annealing mentioned in (b) caused the $\alpha$'s to increase by factors as large as 3000. In addition, an almost complete "erasure" of $\alpha_\parallel$ was accomplished by cooling a $z \parallel z'$ sample through the Néel temperature in the presence of a 60-cycle/sec magnetic field.

All these observations may be interpreted by postulating the existence of antiferromagnetic "domains." As to the specific nature of the domain structure, we tentatively suggest that in the case of $Cr_2O_3$, there are two kinds of domains and that they are characterized, respectively, by each spin in a domain pointing toward, or away from, the nearest oxygen plane which is perpendicular to the $c$ axis. The difference between these two kinds of domains results from the asymmetry of the $Cr^{+++}$ sites with respect to the oxygen planes. This asymmetry produces linear terms in the crystalline electric potential, and in a possible mechanism[6] of the ME effects these terms play an essential role and determine the signs of the $\alpha$'s. Consequently, the suggested domain structure explains the fact that the observed $\alpha$'s can have either sign and that (due to partial cancellations resulting from the presence of two types of domains) they can have variations in their magnitudes. Since the two kinds of domains differ solely by a 180° reversal of all spins, it is clear that the intrinsic $\alpha$'s associated with each domain should have the same temperature dependence. Thus we have a natural explanation of the striking fact that the temperature dependence of each observed $\alpha_\theta$ does not vary even though its sign and magnitude may vary. Finally, we note that the large increases in the magnitudes of the $\alpha$'s which can be produced by magnetic annealing from a temperature just above the Néel point are difficult to explain without postulating antiferromagnetic domains.

We wish to thank Miss J. W. Radue and Mr. M. J. Marrone for help in taking some of the data.

---

[1]D. N. Astrov, J. Exptl. Theoret. Phys. (U.S.S.R.) 38, 984 (1960) [translation: Soviet Phys.-JETP 11, 708 (1960)].

[2]V. J. Folen, G. T. Rado, and E. W. Stalder, Phys. Rev. Letters 6, 607 (1961).

[3]L. D. Landau and E. M. Lifshitz, Electrodynamics of Continuous Media (Addison-Wesley Publishing Company, Inc., Reading, Massachusetts, 1960), p.119. (English translation of a 1958 Russian edition.)

[4]I. E. Dzyaloshinskii, J. Exptl. Theoret. Phys. (U.S.S.R.) 37, 881 (1959) [translation: Soviet Phys.-JETP 10, 628 (1960)].

[5]L. Néel, Proceedings of the International Conference of Theoretical Physics, Kyoto and Tokyo, 1953 (Science Council of Japan, Tokyo, 1954), pp. 701-714; Y. Y. Li, Phys. Rev. 101, 1450 (1956); J. W. Cahn and R. Kikuchi, J. Phys. Chem. Solids 20, 94 (1961).

[6]G. T. Rado, Phys. Rev. Letters 6, 609 (1961).

# EXCITATION OF SPIN-WAVE RESONANCE BY MICROWAVE PHONONS

M. Pomerantz
Thomas J. Watson Research Center, International Business Machines Corporation, Yorktown Heights, New York
(Received September 19, 1961)

The interaction of acoustic vibrations with the spin waves in ferromagnetic media has been treated theoretically by Akhiezer,[1] Kittel and Abrahams,[2] and others[3] in connection with ferromagnetic relaxation times. Their work showed that in the scattering process of a single phonon with a single spin wave (magnon), both energy and linear momentum were conserved. Turner[4] has observed that the linewidths of certain spin waves in YIG are anomalously large, which he attributes to the fact that these spin waves have the same frequencies and wavelengths as some phonons, and hence interact strongly with these phonons and relax more rapidly that other spin waves.

It is not obvious that the theories which were derived for bulk insulating ferromagnets need apply to the case of thin films. Near the surface of the material there is no translational invariance perpendicular to the surface so that linear momentum need not be conserved in this direction. Thus, for films whose thickness is on the order of the magnon wavelength or the acoustic wavelength, one might expect that it is not necessary that the phonon wavelength equal the magnon wavelength in order that interaction occur. To verify these ideas experimentally we have shown directly that a series of standing spin waves can be excited by phonons whose frequency equals that of the spin waves, but whose wavelength is considerably larger than the magnon wavelengths.

The most direct means of observing spin waves is by the method of spin-wave resonance. As explained by Kittel[5] and observed by Seavey and Tannenwald,[6] the pinning of spins at the surfaces of a film will allow the excitation of standing spin waves by uniform fields. These spin waves precess at a frequency given by

$$\omega=\gamma(H-4\pi M)+2A\gamma k^2/M, \qquad (1)$$

when the external magnetic field $\vec{H}$ and the wave vector $\vec{k}$ are perpendicular to the film surface. Hence $\gamma$ = gyromagnetic ratio, $M$ = saturation magnetization, $A$ = exchange constant, $k$ = magnon wave number $= p\pi/L$, where $L$ = film thickness and $p$ is an odd integer. The experiment (similar in technique to one reported by Bömmel and Dransfeld)[7] was performed to detect the excitation of these spin waves by phonons.

A film of Permalloy (80% Ni-20% Fe) of thickness 2600 A was evaporated onto the end of an $AC$-cut quartz cylinder. This end of the cylinder was placed in the magnetic field region of a rectangular microwave cavity resonant at 8.9 kMc/sec at 4.2°K. The other end of the rod was situated in the electric field region of a re-entrant cavity that was resonant at the same frequency. First, the spin-wave spectrum of the film was measured by using the rectangular cavity as part of a microwave spectrometer. Six strong absorption lines were observed. When these lines were fitted by the dispersion relation (1) they were found to correspond to the resonances for $p=0$, 9, 11, 13, 15, and 17. Apparently the spin-wave modes $p=1$ through 7 are strongly attenuated, possibly by eddy current damping.[8] Then the spectrometer was removed and a superheterodyne receiver suitable for receiving weak pulses was connected to the rectangular cavity. By pulsing the re-entrant cavity with 10 watts of power of 1-$\mu$sec pulse width, transverse phonons were initiated in the quartz bar. These propagated down the bar and entered the film which was now in a quiescent cavity. The power in the rectangular cavity was observed as a function of magnetic field. Power was observed at those values of the field at which electromagnetically excited spin-wave resonances had previously been observed. Thus, the microwave phonons had excited the magnetization into precession in the several spin-wave modes, and at resonance the precessing magnetization produced measurable excitation of the cavity.

This demonstrates that phonons of frequency 8.9 kMc/sec and wavelength ≈3400 A interact with spin waves of the same frequency and with a number of different wavelengths, all less than 1000 A. Only four of the spin waves were sufficiently strongly excited acoustically to be observed. The relative amplitudes of the power output at the acoustically excited lines were 1:0.25:0.12:0.05. When observed by electromagnetic excitation the relative amplitudes of the first four lines were 1:0.29:0.37:0.13. This indicates that the relative phonon excitation is increased as the acoustic and magnon wavelengths approach equality.

The theoretical expectation[2] is that phonons are coupled to spin waves via a magnetoelastic energy that is also responsible for magnetostriction. In order to investigate this, experiments similar to

the one described above were performed on two films whose magnetostriction constants, $\lambda$, were considerably different. The average magnetostrictive constants of 83Ni17Fe Permalloy[9] are approximately zero, but the average magnetostriction of the composition 76Ni24Fe is $\lambda \approx 10 \times 10^{-6}$, which is greater than that of 83-17 Permalloy by at least a factor of ten. A sample was prepared by evaporating a film of 83-17 Permalloy onto one half of the end surface of an $AC$-cut quartz rod. A 76-24 Permalloy film was evaporated on the other half of the same surface. (This was done to assure that the same amount of phonon power entered each film.) The thicknesses of the films were made as nearly equal as possible, 2270 A for the 76-24 Permalloy and 2400 A for the 83-17 Permalloy. The electromagnetically excited ferromagnetic resonance of this compound sample showed two distinct spin-wave spectra corresponding to the two "half-moon" shaped films. Because the $4\pi M$ of the two samples differ by more than a thousand gauss the spectra do not overlap. The amplitudes and linewidths of the main ($k = 0$) lines were approximately the same for both compositions when the resonances were excited electromagnetically. The phonon-excited resonances were quite different, however. It was found that spin-wave resonance was excited in the 76-24 Permalloy (which has the larger magnetostriction), but to our experimental sensitivity no ferromagnetic resonance was excited in the 83-17 Permalloy. The phonon spin-wave interaction was at least a factor of 15 greater in the 76-24 Permalloy than in the 83-17 Permalloy. It is unlikely that the small difference in film thickness has a large effect on the excitation; the interaction of magnons and phonons seems directly related to the magnetostriction.

From these results some qualitative conclusions can be drawn about the relaxation processes in Permalloy films. The spin-phonon interaction was shown to be strongly dependent on the magnetostriction of the films near the 80-20 composition, yet the linewidths of the resonances were approximately the same (≈40 gauss) for all compositions studied. This means that spin-phonon processes cannot be the major source of the linewidths; there are apparently more rapid processes shortening the lifetime of the spins. This lends further experimental support to the conclusions of Kittel and Abrahams[2] and Bloembergen and Wang[10] that direct spin-lattice interactions are not the most important source of linewidths in ferromagnetic metals at temperatures well below the Curie temperature.

It is a pleasure to acknowledge helpful conversations with R. Landauer, A. H. Nethercot, Jr., and P. Seiden. We are indebted to W. Kately for film preparations, and to I. L. Gelles for help with the microwave spectroscopy. Particular thanks are due J. P. Anderson for his able and enthusiastic technical support.

[1]A. Akhiezer, J. Phys. (U.S.S.R.) 10, 217 (1946).
[2]C. Kittel and E. Abrahams, Revs. Modern Phys. 25, 233 (1953).
[3]The work of the Russian school is reviewed by A. I. Akhiezer, V. G. Bar'yakhtar, and M. I. Kaganov, Uspekhi Fiz. Nauk 71, 533 (1960); 72, 3 (1960) [translations: Soviet Phys. – Uspekhi 3, 567, 661 (1961)].
[4]E. H. Turner, Phys. Rev. Letters 1, 100 (1958).
[5]C. Kittel, Phys. Rev. 110, 1295 (1958).
[6]M. H. Seavey and P. E. Tannenwald, Phys. Rev. Letters 1, 168 (1958).
[7]H. Bömmel and K. Dransfeld, Phys. Rev. Letters 3, 81 (1959).
[8]P. Pincus, Phys. Rev. 118, 658 (1960).
[9]R. M. Bozorth, Revs. Modern Phys. 25, 42 (1953).
[10]N. Bloembergen and S. Wang, Phys. Rev. 93, 72 (1954).

# SILICON DIVACANCY AND ITS DIRECT PRODUCTION BY ELECTRON IRRADIATION

J. W. Corbett and G. D. Watkins
General Electric Research Laboratory, Schenectady, New York
(Received September 19, 1961)

To date two defects produced in radiation damage of silicon have been identified.[1,2] These defects are a vacancy-oxygen pair and a vacancy-phosphorous pair. They were identified largely by their associated electron spin resonance spectra and have been labeled the Si-*A* and Si-*E* centers, respectively. The studies associated with these identifications demonstrated that the vacancy is mobile in a room-temperature irradiation experiment and emphasized the importance of impurities in influencing the radiation-damage processes. In this Letter we report the identification of an intrinsic defect, which is stable at room temperature, the divacancy. We also demonstrate that this defect can be produced directly in a high-energy electron irradiation (that is, the migration and agglomeration of vacancies is not required for its formation). In addition, a marked anisotropy is observed in the production rate with respect to the electron beam direction, giving insight into the detailed production process.

The divacancy is shown in Fig. 1. It consists of two vacant, nearest-neighbor, lattice sites, *A* and *B*, each surrounded by three occupied lattice sites, 1-6. The divacancy identification has been made by studies of two associated electron spin resonance spectra, previously designated the Si-*J* and the Si-*C* centers.[2] These spectra are interpreted as arising as follows: The electrons on atoms 2 and 3 and on atoms 5 and 6 each pair in molecular bonds as shown in the figure. The Si-*J* center is observed in *p*-type material and is interpreted as arising from a single unpaired electron in the extended orbital between atoms 1 and 4. In this state, the divacancy is a singly ionized donor. The Si-*C* center is observed in high-resistivity silicon and is interpreted as arising from a third electron in the antibonding orbital between atoms 1 and 4, the two bonding orbitals being filled. In this state the divacancy is a singly ionized acceptor. The Si-*C* center is not observed in low-resistivity *n*-type material, indicating that the divacancy can also accept an additional electron. It thus can act as both a single donor and a double acceptor.

Some of the arguments leading to this identification are summarized briefly as follows:

1. These spectra have anisotropic *g* tensors as shown in Table I. Both spectra exhibit resolved, axially symmetric, hyperfine interactions with two equivalent silicon atoms. The hyperfine constants are also shown in Table I. The resonance-electron orbital between atoms 1 and 4 (see Fig. 1) accounts for the simple ⟨111⟩ hyperfine interactions with the same axis for two silicon atoms, while the *g* tensor, reflecting the symmetry of the wave function as a whole, is tilted away from this direction.

2. For the divacancy shown in Fig. 1, in addi-

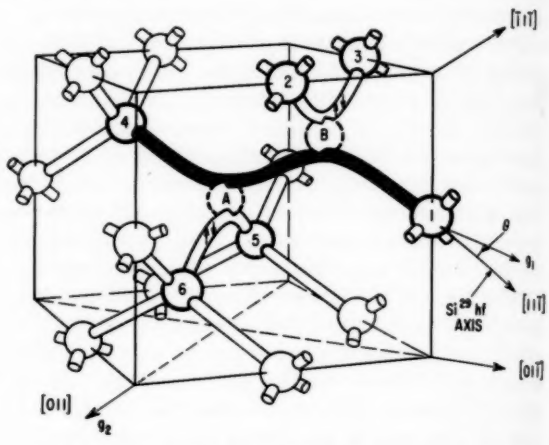


FIG. 1. The silicon divacancy. The dashed circles labeled *A* and *B* represent the two adjacent vacant lattice sites. The electrons associated with the defect can be regarded as forming the bonds shown in the figure. The axes for the spin-resonance data in Table I are indicated in the figure.

Table I. Spin Hamiltonian constants for the divacancy spectra (see Fig. 1).

| Spectrum | $g(\pm 0.0003)$ | $\theta$ (See Fig. 1) | $Si^{29}$ hf ($10^{-4}$ cm$^{-1}$) |
|---|---|---|---|
| Si-*C* | $g_1 = 2.0012$ | | |
| | $g_2 = 2.0135$ | $6 \pm 1°$ | $A_\parallel = 79 \pm 2$ |
| | $g_3 = 2.0150$ | | $A_\perp = 56 \pm 2$ |
| Si-*J* | $g_1 = 2.0004$ | | |
| | $g_2 = 2.0020$ | $7.7 \pm 0.5°$ | $A_\parallel = 67.8 \pm 0.5$ |
| | $g_3 = 2.0041$ | | $A_\perp = 40.0 \pm 0.5$ |

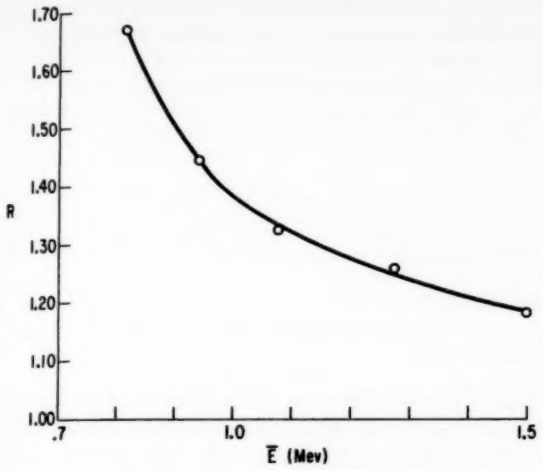


FIG. 2. $R$ vs the average energy of the incident electron beam, $\bar{E}$. $R$ is the ratio of the number of divacancies with the vacancy-vacancy direction along the incident beam ⟨111⟩ direction (say the $[\bar{1}1\bar{1}]$ of Fig. 1) to the number along one of the other three equivalent ⟨111⟩ directions (the $[11\bar{1}]$).

tion to the orbital between atoms 1 and 4, as shown, equally likely configurations involve the orbital being between atoms 2 and 5 and between atoms 3 and 6. For both the Si-$C$ and Si-$J$ centers, motion between these configurations has been detected both by stress-induced alignment and by linewidth studies, confirming this prediction of the model. The activation energy for this motion is ~0.06 ev for both centers.

3. Preferential alignment of the vacancy-vacancy direction has been quenched in by stressing at elevated temperatures. The magnitude of the alignment as well as the kinetics of reorientation is identical as monitored by both centers. The activation energy for this motion is ~1.3 ev.

4. Both spectra are observed after an in situ irradiation at 20°K, showing that they are due to a primary defect, which does not require annealing for formation.

That the divacancy is produced as a primary process has also been demonstrated in an informative way as follows:

Oriented samples 0.010 in. × 0.1 in. × 0.6 in. were cut from $p$-type (~$3\times10^{16}$ B/cc) pulled silicon with the thin dimension a ⟨110⟩ direction. For convenience we will consider this thin dimension to be the $[01\bar{1}]$ of Fig. 1. These samples were irradiated at room temperature with a high-energy electron beam incident along the $[\bar{1}1\bar{1}]$ direction, and the Si-$J$ center resonance observed. By observing the relative intensities of the multiplets of the spin resonance spectrum it is possible to count the divacancies in each of the possible orientations. The ratio, $R$, of the number with the vacancy-vacancy axis along the beam direction ($[\bar{1}1\bar{1}]$) to the number in one of the other three equivalent ⟨111⟩ directions (i.e., $[11\bar{1}]$) is shown in Fig. 2 as a function of bombarding energy. As can be seen, there is a substantial anisotropy in the production rate, which increases with decreasing bombarding energy.

This behavior can be qualitatively understood in terms of a conventional model for divacancy production: A high-energy electron collides with the nucleus of an atom and imparts a recoil energy to the atom. The recoiling atom collides with a nearest neighbor atom, causing it to be displaced into the lattice as an interstitial. In addition the initial recoil atom must retain enough energy so that it too becomes an interstitial. In this way, two adjacent vacancies, a divacancy, are created. The energy the primary recoil atom receives in the collision with a high-energy electron, and the direction of recoil are correlated, being determined by the Mott-Rutherford scattering formula. The highest energy recoil is along the beam direction. Consequently as the beam energy is reduced, a point is ultimately reached where sufficient recoil energy is available to produce a divacancy along the beam direction but not in the ⟨111⟩ direction 70° 32′ away from the beam direction, which suggests the tendency seen in Fig. 2.

There are several considerations which make the data in Fig. 2 provisional (e.g., local heating of the lattice during the defect production process, finite sample thickness, and the fact that the irradiation was at a temperature where single vacancies could aggregate). However, all of these would reduce the observed anisotropy, so that it is at least as large as shown in Fig. 2.

In summary we observe the divacancy as the result of the direct production process. It is produced at a rate ~5% of the vacancy production rate, as monitored by the Si-$A$ center, for a 1.5-Mev irradiation,[3] and plays an important part in room-temperature radiation-damage processes.

---

[1]G. D. Watkins and J. W. Corbett, Phys. Rev. 121, 1001 (1961); J. W. Corbett, G. D. Watkins, R. M. Chrenko, and R. S. McDonald, Phys. Rev. 121, 1015 (1961).

[2]G. D. Watkins and J. W. Corbett, Discussions Faraday Soc. (to be published).

[3]Analysis of the absolute production rates vs bombarding energy for the Si-$J$ center indicates a considerably higher threshold energy for divacancy production than that for the single vacancy, as is to be expected. This is in agreement with work by Bemski (to be published), who similarly reports a higher threshold energy for the Si-$C$ center formation. As a result of this observation, Bemski independently concluded that the Si-$C$ center was to be associated with a multiple defect, suggesting the divacancy as a possibility.

## BOUND EXCITON COMPLEXES

D. G. Thomas and J. J. Hopfield
Bell Telephone Laboratories, Murray Hill, New Jersey
(Received September 11, 1961)

Exciton complexes in which excitons are bound to neutral or charged donors or acceptors have been described by Haynes[1] and Lampert.[2] In crystals with a direct band gap, such states are observable as sharp absorption and emission lines occurring at wavelengths longer than that of the lowest energy intrinsic exciton state. This Letter shows that the Zeeman effect of these impurity complex states can be used to identify which type of center a given absorption line represents. In this way, the $g$ values of donors and acceptors, the binding energies of the various complexes, and even information about the energy levels and $g$ values of excited states of donors and acceptors can be obtained. The electron-hole spin-spin (exchange) interaction can be measured in some of these states. The experimental results discussed are for CdS, but the method of investigation seems to be promising for a wide class of semiconducting crystals. Previous work has established the energies of the intrinsic exciton lines[3] in CdS, but the explanation of the lines occurring at lower energies has remained unsatisfactory.[4,5]

Excitons can be bound to neutral donors or acceptors to form molecular states, or to ionized donors or acceptors to form molecular ion states, as illustrated in Fig. 1. The neutral donors and acceptors are doublet states ($S=\frac{1}{2}$), and this is also true for the complexes formed from these states since the "bonding" electrons or holes must have antiparallel spins. (It is well known that for molecular hydrogen, if the "bonding" particles have parallel spins an unstable system results. Precisely the same considerations apply to the exciton complexes discussed here.) The states considered here are ground states and so have no orbital angular momentum. In a magnetic field the states derived from the neutral centers will split, as shown in Fig. 1, with a $g$ value equal to that of the odd particle in the particular complex. This four-level system gives rise to two pairs of lines, one with a separation controlled by $|g_u - g_l|$ and the other controlled by $|g_u + g_l|$, where $u$ and $l$ refer to the upper and lower states, respectively.

In hexagonal CdS free electrons occupy an $S$-like $J=\frac{1}{2}$ $\Gamma_7$ band, and free holes (from the top valence band) a $P$-like $J=\frac{3}{2}$ $\Gamma_9$ band.[3] The free electron has an almost isotropic $g$ value of $-1.7_8$. Because the conduction band is simple, this $g$ value will be almost independent of the binding of the electron in a center. Symmetry requires that the $g$

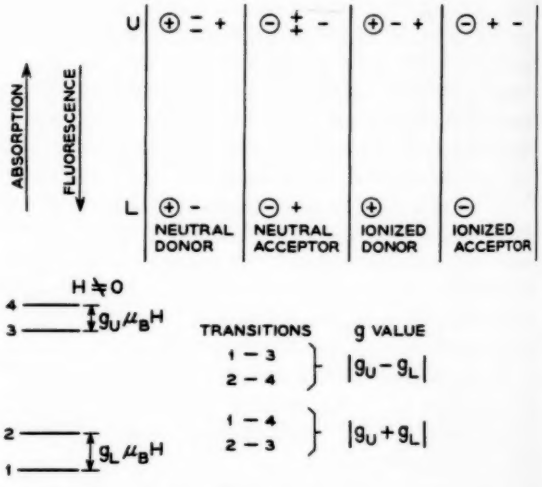


FIG. 1. Schematic diagram illustrating the ground and excited states of the various transitions discussed in the text. The $g$ values of the states arising from the neutral centers are determined by the $g$ value of the odd particle, and the splittings of these states are as illustrated. The ionized centers show no splitting in the ground states; the splitting of the excited states of these centers with $c \perp H$ is complicated by the presence of a spin-spin interaction energy. The charges within a circle indicate a chemical center.

Table I. CdS – 1.6°K.

| Line | Energy (ev) | Energy below exciton $A$(2.5537 ev) (ev) |
|---|---|---|
| $I_1$ | 2.53595 (4888.5 A) | 0.0177 |
| $I_2$ | 2.5471 (4867.15 A) | 0.0066 |
| $I_3$ | 2.5499 (4861.7 A) | 0.0038 |

value of the hole has the form

$$g_h = g_{h\parallel} \cos\theta,$$

where $\theta$ is the angle between the magnetic field, $H$, and the $c$ axis. The hole, belonging to a rather complicated and almost degenerate valence band structure, can have a $g$ value sensitive to its exact state of binding. For the free hole, $g_{h\parallel} = -1.1_5$. For $c\parallel H$ selection rules show that the 1-3 and 2-4 transitions will occur optically, resulting in a doublet split with a $g$ value of $|g_u - g_l|$. At an arbitrary value of $\theta$, however, mixing of the states occurs, and a full quartet of lines becomes visible. The additional pair is separated with a $g$ value of $|g_u + g_l|$. From measurements of this type it is easy to derive the individual $g$ values.

Our study of "pure" vapor-grown crystals of CdS of thickness 10-100 $\mu$ has been chiefly concerned with three prominent sharp lines listed in Table I. These lines are strongly active for light polarized perpendicular to the $c$ axis, which is also the polarization of the lowest energy exciton, exciton $A$. At 1.6°K in selected crystals the lines may have a width of 0.6 $cm^{-1}$ or less. They can be seen at 20°K but not at 77°K. $I_1$ and $I_2$ are readily seen in both absorption and fluorescence, while $I_3$ is observed in absorption. $I_1$ is absent in some crystals. Sometimes other lines appear near $I_2$, the whole group behaving similarly in a magnetic field. Additional lines also often occur near $I_3$; some of these behave like $I_3$ in a magnetic field while others behave like $I_2$. Many other lines occur, prominent among which are comparatively broad lines (about 6 $cm^{-1}$ wide) seen in fluorescence at photon energies below $I_1$; some of these correspond to emission taking place with phonon creation.

Lines $I_1$ and $I_2$ exhibit linear Zeeman splittings which can conveniently be studied in fluorescence. The splittings of $I_1$ and $I_2$ as a function of $\cos\theta$ are plotted in Fig. 2 for $H = 31\,000$ gauss. Quartets are seen when $\theta$ has values other than 0° and 90°. Within experimental error there is a linear dependence between the splittings and $\cos\theta$, so the relations

$$g_e \pm g_h = g_{e0} \pm g_{h\parallel} \cos\theta$$

must hold, where $g_{e0}$ is an isotropic electron $g$ value equal to -1.7$_6$ for $I_1$, and -1.7$_1$ for $I_2$. For $I_2$, $g_{h\parallel}$ equals -1.7; and for $I_1$, $g_{h\parallel}$ equals -2.7$_6$. It happens that $g_{h\parallel} \approx g_{e0}$ for $I_2$. This near equality is the reason that for $c\parallel H$, with the splitting determined by $g_{e0} - g_{h\parallel}$, no Zeeman effect is observed for this line.[5]

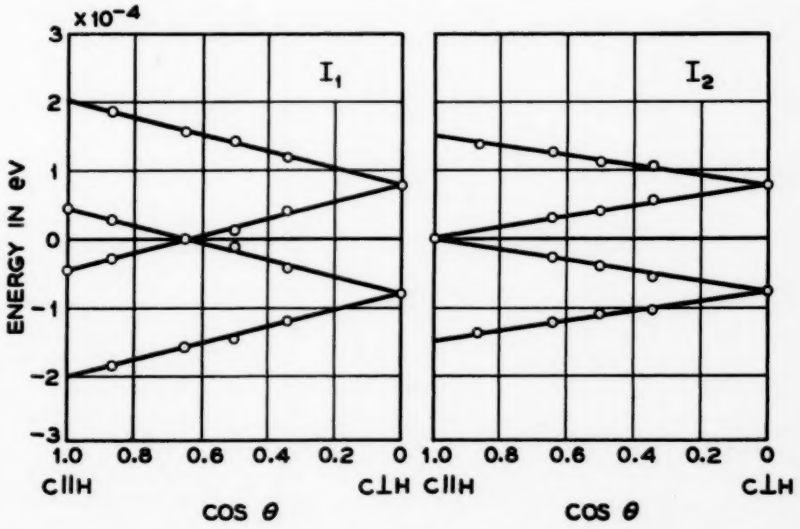


FIG. 2. Splitting of lines $I_1$ and $I_2$ at 31 000 gauss as a function of $\cos\theta$ at 1.6°K, as seen in fluorescence. Notice that when $\theta \neq 0°$ or $\theta \neq 90°$, quartets occur. The zero of energy is taken to be at the center of each group of lines.

When $I_1$ and $I_2$ are observed in absorption for $c \| H$ and $c \perp H$, the two lines in a pair sometimes have different strengths. The differences in strength increase as the magnetic splittings increase or as the temperature decreases, indicating that, for the experimental conditions used, thermal equilibrium of the spins is being approached in the lower states of the complexes. The results are as follows:

| | $I_1$ | $I_2$ |
|---|---|---|
| $c \| H$ | High-energy line strong | No splitting observable |
| $c \perp H$ | Both lines equal in strength | High-energy line strong |

It is clear that for $c \perp H$ there is thermalization in the lower state of line $I_2$, but that this does not occur for line $I_1$. Since $g_{e0} = -1.7_6$ and $g_{h\perp} = 0$, $I_2$ must arise from a neutral donor, and $I_1$ from a neutral acceptor. The thermalization results for $c \| H$ are consistent with these conclusions when it is remembered that for $I_2$, $g_{h\|} \approx g_{e0}$, and that for $I_1$, $|g_{h\|}| > |g_{e0}|$. It is interesting to note that the free hole has $g = -1.1_5$, but that in the exciton complex $\oplus = +$ the value has increased to -1.7, and in the neutral acceptor it is $-2.7_6$.

It follows that the other lines described above, which behave magnetically like $I_2$ also arise from donor states which are, however, chemically different from the center responsible for line $I_2$. In a similar way, the other lines which behave like $I_3$ must, as described below, be molecular ion states derived from chemically different centers. It is an interesting fact that we have seen no other lines which behave like $I_1$. This may be because there is only one acceptor state present in appreciable quantity, but it seems more probable that this is the only "shallow" acceptor state present; deeper lying acceptor states probably give rise to much broader lines as a result of stronger coupling to the acoustic phonons of the lattice.

The fluorescent intensities of $I_1$ and $I_2$ show that spin thermalization is not occurring in the upper states, presumably because of the short lifetime of these states.

CdS is normally *n* type, so acceptors are therefore usually compensated (ionized). On illumination with band gap light, however, free holes and electrons are made. These can be trapped at low temperatures by the ionized acceptor and donors, respectively, to form neutral centers on which the exciton complexes can be formed. It is found that when the lines are observed in absorption using as little band gap light as possible, infrared illumination of the crystal causes $I_1$ and $I_2$ to diminish in strength (and in some cases to vanish), while $I_3$ increases markedly in strength. Since the infrared illumination is of such a wavelength as to ionize the acceptor preferentially, we may conclude that this occurs and that the free hole then ionizes the donors. Thus, the neutral donor and acceptor concentrations are decreased while those of the ionized states are increased. We may therefore conclude that $I_3$ corresponds to the formation of a molecular ion state.

The magnetic behavior of $I_3$, although not simple, appears consistent with its assignment as a molecular ion state. For example, no thermalization is observed for absorption, the expected situation for a singlet ground state. In a magnetic field with $c \perp H$, $I_3$ splits unsymmetrically in the sense that the lines do not shift linearly with $H$; at low fields only the high-energy member of the doublet is visible, but as the field increases the low-energy line is seen with steadily increasing strength. Extrapolation of the positions of the lines to $H = 0$ shows that there is a zero-field splitting of $3.1 \times 10^{-4}$ ev. Symmetry arguments show that with $c \perp H$, states with antiparallel spins ($1S\ \Gamma_5$ states) are mixed with states with parallel spins ($1S\ \Gamma_6$ states). The zero-field splitting is therefore ascribed to a spin-spin interaction energy, and since the transition to the $1S\ \Gamma_6$ state is forbidden, it is clear that this state has an energy lower than the $1S\ \Gamma_5$ state. Such an interaction can occur in absorption lines due to excitons bound to ionized donors or acceptors, where the complex involves an odd number of electrons and of holes. It cannot occur in absorption lines due to excitons bound to neutral donors or acceptors, since the spins of the two like particles will be antiparallel. The spin-spin interaction energy of $3.1 \times 10^{-4}$ ev is surprisingly large. We have, however, evidence from the effect of strain on the intrinsic exciton lines that the free exciton has a similarly large value.

The methods described here could be of help in determining the types of impurities present in many 2-6 semiconductors. Information is also derived about the donors and acceptors, as illustrated here by the determination of the $g$ value of the hole on the acceptor (a value that would be hard to obtain by paramagnetic resonance since $\Delta m = 3$ for a spin transition in the $J = \frac{3}{2}$

band). The dethermalization of the lower state population by microwave pumping should be easily detected optically. Donor and perhaps acceptor $g$ values can therefore be measured with microwave precision on crystals too small to investigate with normal microwave techniques. Finally, there is evidence in the fluorescent spectra for transitions which leave neutral donors or acceptors in excited states. Such transitions provide a means of measuring donor and acceptor excited state energies and magnetic splittings.

[1]J. R. Haynes, Phys. Rev. Letters 4, 361 (1960).
[2]M. A. Lampert, Phys. Rev. Letters 1, 450 (1958).
[3]J. J. Hopfield and D. G. Thomas, Phys. Rev. 122, 35 (1961).
[4]L. S. Pedrotti and D. C. Reynolds, Phys. Rev. 120, 1664 (1960).
[5]R. G. Wheeler and J. O. Dimmock, Phys. Rev. Letters 3, 372 (1959).

## $M$-SHELL, RELATIVISTIC ELECTRON WAVE FUNCTIONS*

H. R. Brewer, D. S. Harmer, and D. H. Hay
Georgia Institute of Technology, Atlanta, Georgia
(Received August 3, 1961)

The effects of screening and finite nuclear size on $M$-shell electron wave functions have been calculated numerically. The ratio of the corrected $M$-shell wave functions to the corresponding point-nuclear values (evaluated at the finite nuclear radius) is presented here in Fig. 1 for their application in evaluating $M$-capture transition probabilities.[1,2] In the past, these orbital capture transitions were corrected empirically for screening. The results presented here indicate the necessity for including such corrections and, in addition, indicate wide variations between the correction factors for different $M$ subshells.

The correction factors were derived from wave functions which were calculated as part of a program for obtaining $M$-shell internal conversion coefficients. The wave functions are available in tabular form[3] for points outside the nuclear surface for atomic numbers 55 through 90 in steps of 5.

For the evaluation of these wave functions, a uniform charge distribution was assumed inside the nucleus, and power series solutions[4] were obtained for $f$ and $g$ (small and large component) of Dirac's equations. These series solutions were evaluated at the nuclear radius[5] to give starting values for a numerical solution of the equations in the external region. Here the potential due to the nucleus and orbital electrons was represented by a Thomas-Fermi-Dirac (TFD) potential[6] and is given by

$$V = \alpha Z \varphi / r + D.$$

In this equation $\alpha$ is the fine structure constant, $\varphi$ is the screening function taken from Umeda's tables,[7] $D$ is the Dirac exchange term,[6] $Z$ is the atomic number, and $r$ is the radial distance. The outer boundary condition for $f(a)$ and $g(a)$ is given by

$$f(a)/g(a) = -[(1-W)/(1+W)]^{1/2},$$

where $W$ is the trial energy eigenvalue and $a$ is the value of $r$ for which $\varphi$ vanishes. Trial values of $W$ were varied until the solutions matched both the boundary condition at $r=a$ and that at the nuclear surface, and possessed the correct number of nodes in the interval.

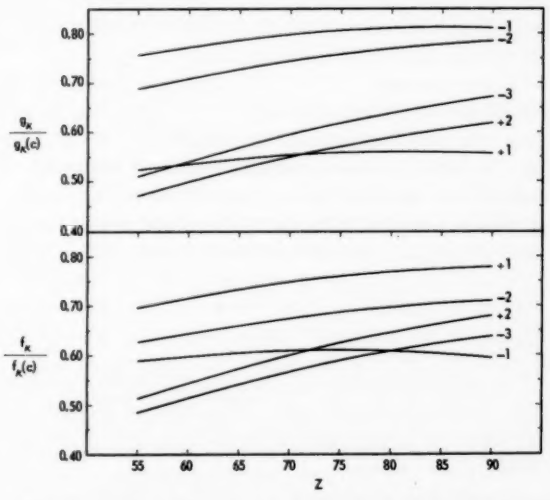


FIG. 1. $f_\kappa/f_\kappa(c)$ and $g_\kappa/g_\kappa(c)$ are the ratios of the screened, finite nuclear size functions to the corresponding analytic point-nuclear functions[7] evaluated at the nuclear radius and plotted as a function of the nuclear charge $Z$. The numbers tc the right of each curve give the value of $\kappa$ as defined in the text.

Table I. Energy levels for $M$-shell electrons computed with finite size and TFD screening corrections compared with experimental and Coulomb point-nuclear values.

| $Z$ | $A$ | $\kappa$ | (Subshell) | $W$ ($mc^2$) | $(1-W)$ Calculated (ev) | $(1-W)$ Experimental[a] (ev) | $(1-W)$ Coulomb point nucleus (ev) |
|---|---|---|---|---|---|---|---|
| 55 | 138 | -3 | $M_{V}$ | 0.998542 | 745 | 720 | 4594 |
| | | +2 | $M_{IV}$ | 0.998511 | 760 | 738 | 4636 |
| | | -2 | $M_{III}$ | 0.998014 | 1014 | 1001 | 4636 |
| | | +1 | $M_{II}$ | 0.997868 | 1089 | 1070 | 4773 |
| | | -1 | $M_{I}$ | 0.997612 | 1220 | 1217 | 4773 |
| 90 | 228 | -3 | $M_{V}$ | 0.992863 | 3646 | 3333 | 12 395 |
| | | +2 | $M_{IV}$ | 0.992501 | 3831 | 3475 | 12 712 |
| | | -2 | $M_{III}$ | 0.991493 | 4346 | 4045 | 12 712 |
| | | +1 | $M_{II}$ | 0.989854 | 5184 | 4828 | 13 937 |
| | | -1 | $M_{I}$ | 0.989251 | 5492 | 5181 | 13 937 |

[a]See reference 9.

Figure 1 shows the ratio of screened, finite-nuclear-size $f$ and $g$ to their corresponding Coulomb, point-nuclear values[8] at the nuclear radius. The calculation errors (truncation and round-off) in $f$ and $g$ are believed to be less than 0.5%. These were estimated by inserting a Coulomb potential in place of the screened one and beginning the numerical integration at the nucleus with the Coulomb, point-nuclear starting values. The results were then compared with the analytic solutions[8] to obtain the error estimate above.

A comparison of the TFD energy levels with the Coulomb and experimental values[9] is given in Table I for the highest and lowest values of $Z$. The deviations between computed and experimental values for intermediate $Z$ lay in between those given in Table I. The symbol $\kappa$ used to designate the levels has the conventional meaning[1]:

$$\kappa = -(l+1) \text{ when } j = l + \tfrac{1}{2},$$

$$\kappa = \quad l \quad \text{ when } j = l - \tfrac{1}{2}.$$

The correspondence of the experimental and computed energy levels over this range of $Z$ lends confidence to the use of the TFD screened potential.

In conclusion the authors wish to thank Dr. M. E. Rose for suggesting the problem and for his kind assistance during the course of the work.

---

*Work supported in part by the National Science Foundation.

[1]H. Brysk and M. E. Rose, Revs. Modern Phys. 30, 1169 (1958).

[2]B. L. Robinson and R. W. Fink, Revs. Modern Phys. 32, 117 (1960).

[3]These tables have been deposited as Document number 6855 with the ADI Auxiliary Publications Project, Photoduplication Service, Library of Congress, Washington 25, D. C. A copy may be secured by citing the Document number and by remitting $60.00 for photoprints, or $9.25 for 35 mm microfilm. Advance payment is required. Make checks or money orders payable to: Chief, Photoduplication Service, Library of Congress.

[4]H. Brysk and M. E. Rose, Oak Ridge National Laboratory No. 1830 (unpublished).

[5]The value $1.2 \times A^{1/3}$ fermis was used for the nuclear radius.

[6]L. Brillouin, Actualités sci. et ind. No. 160 (1934).

[7]K. Umeda, J. Fac. Sci., Hokkaido Univ. 3, 171 (1942).

[8]W. B. Payne, Ph.D. thesis, Louisiana State University, 1955 (unpublished).

[9]A. E. Sandström, Encyclopedia of Physics, edited by S. Flügge (Springer-Verlag, Berlin, 1957), Vol. 30, p. 226.

# ELECTRON-ION RECOMBINATION COEFFICIENTS IN NITROGEN AND IN OXYGEN*

W. H. Kasner, W. A. Rogers,† and M. A. Biondi‡
Westinghouse Research Laboratories, Pittsburgh, Pennsylvania
(Received September 22, 1961)

Currently, there is considerable interest in predicting free-electron lifetimes in various regions of the ionosphere following ionizing events, such as solar flares. An important process in determining the electron loss is recombination between electrons and the positive ions present in the upper atmosphere. It has been reasonably well established from analysis of ionospheric observations[1] and from laboratory experiments[2,3] that the recombination coefficient $\alpha$ (defined by $dn_e/dt = -\alpha n_e n_+$, where $n_e$ and $n_+$ are the electron and positive ion densities, respectively) may be as large as $10^{-8}$ to $10^{-6}$ cm$^3$/sec and that the capture process is dissociative recombination.[4]

Since no adequate theoretical calculations of the rate of the dissociative recombination reaction,[5] e.g.,

$$(XY)^+ + e \longrightarrow (XY)^* \xrightarrow[\text{unstable}]{} X^* + Y, \quad (1)$$

are available, appeal is generally made to laboratory measurements of the recombination coefficients in atmospheric gases.[2,6] Unfortunately, previous measurements were made without identification of the ions responsible for the recombination and under conditions where more complex ion types, e.g., $O_3^+$ in oxygen and $N_3^+$ and $N_4^+$ in nitrogen, are observed. This Letter presents the preliminary results of an experiment involving microwave determinations of the decay of electron density during the afterglow following ionization of gas in a cavity,[7] coupled with the simultaneous identification, by an rf-type mass spectrometer, of the afterglow positive ion currents to a wall of the cavity. From these measurements, recombination coefficients appropriate to particular positive ion species, e.g., $N_2^+$, can be assigned.

The apparatus consists of a rectangular, stainless steel, microwave cavity containing in one wall a quartz iris for coupling microwave energy, in the opposite wall a 0.008-inch diameter effusion orifice leading to a Boyd-type[8] rf mass spectrometer and its differential pumping system, in a third wall an optical viewing port, and in a fourth wall a lead to an ultra-high vacuum, gas-handling system. The gas-handling system, the cavity, and the mass spectrometer differential pumping system are baked at 350°C for 14 hours to minimize impurity effects. The high-purity gas samples, contained in steel pressure tanks,[9] are fed into the system through controlled leaks.

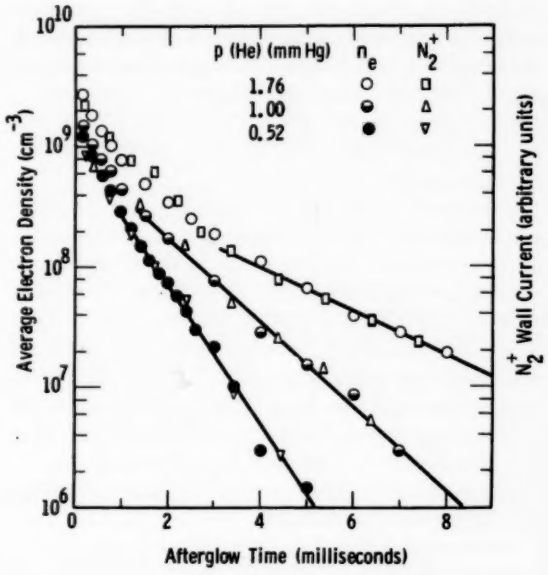


FIG. 1. Electron and $N_2^+$ ion decay in the afterglow of $N_2$-He microwave discharges having constant nitrogen pressure, 0.006 mm Hg, and variable helium pressure. The $N_2^+$ wall currents are normalized to the respective electron density decay curves at an afterglow time of approximately 2 milliseconds.

In order to carry out measurements at low concentrations of nitrogen or oxygen, an inert buffer gas is used to inhibit particle loss by diffusion to the walls. It was observed that in either pure nitrogen or nitrogen-helium mixtures, the predominant afterglow ions for nitrogen pressures in the range 0.1 to 7.0 mm Hg were $N_3^+$ and $N_4^+$, while at nitrogen pressures less than 0.01 mm Hg, $N_2^+$ was the only significant ion in the afterglow.[10] Similarly, in oxygen, at partial pressures of less than 0.005 mm Hg, $O_2^+$ predominated.

At low total pressures, see Fig. 1, the predominant loss of electrons and $N_2^+$ ions in the late afterglow is by ambipolar diffusion to the walls, as indicated by the fact that the rate of particle loss varies inversely with gas pressure and exponentially with time. The curvature in the top curve shows significant electron-ion recombina-

tion in the early afterglow. From the known fundamental diffusion length of the cavity, $\Lambda = 1.126$ cm, a $D_a p$ value of approximately 900 (cm²/sec) × (mm Hg) is obtained for $N_2^+$ ions and electrons moving in helium. At this low partial pressure of nitrogen, 0.006 mm Hg, $N_3^+$ and $N_4^+$ ions are essentially absent. The decay of the normalized wall current of $N_2^+$ ions (which, for fundamental mode diffusion, is proportional to the average density of $N_2^+$ inside the cavity) follows the average electron density, within the accuracy of the present measurements.[11]

In order to study recombination under conditions where diffusion loss is unimportant, it is necessary to increase the pressure of the buffer gas to reduce the diffusion rate. Neon is more suitable than helium, the gas conventionally used,[6,12] since, at a given pressure, neon inhibits diffusion more strongly[13] and effuses into the mass spectrometer more slowly than helium, thus reducing choking of the mass spectrometer pumping system. The ionization potential of neon is sufficiently high that one observes only ions of the minority nitrogen or oxygen constituent.

Measurements of electron-ion recombination have been carried out under conditions where one particular ion species (except for the $N_3^+$-$N_4^+$ combination) predominates during the afterglow. Under these conditions, and when diffusion loss can be neglected, the solution of the electron density equation becomes $(1/n_e) = (1/n_{e0}) + \alpha t$. Examples of data obtained for recombination loss of $N_2^+$ ions and electrons and for $O_2^+$ ions and electrons are shown in Fig. 2. The neon gas pressure is sufficiently high so that the ratio of recombination loss to fundamental mode diffusion loss is large over the entire range, varying from ~200 to ~10 in the data shown. From the initial straight portions of the curves, covering a factor of ~10 in electron density, taken at several neon partial pressures, we obtain the values $\alpha(N_2^+) = (5.9 \pm 1) \times 10^{-7}$ cm³/sec and $\alpha(O_2^+) = (3.8 \pm 1) \times 10^{-7}$ cm³/sec. The uncertainty in these values arises largely from imperfect knowledge of (a) the correction of the recombination curve for diffusion effects in this geometry,[14] (b) the spatial density distribution of the electrons, which affects the determination of absolute electron density from the measured cavity frequency shifts,[7] and (c) the time-resolved afterglow ion currents, which indicate the importance of any other positive ions in the afterglow. Electron attachment in oxygen should not be a significant factor in the recombination analysis, since the oxygen partial pressure was so low,

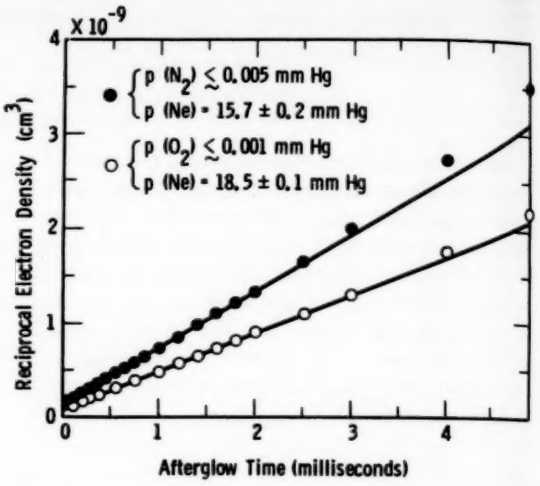


FIG. 2. Time variation of the reciprocal electron density in the afterglow of high-pressure $N_2$-Ne and $O_2$-Ne microwave discharges.

i.e., less than $10^{-3}$ mm Hg.

At higher partial pressures of nitrogen, $N_3^+$ and $N_4^+$ ions appear in nearly equal abundance and seem to vary together with both gas pressure and time during the afterglow. The curves of $1/n_e$ vs time are linear in this case also, indicating an effective recombination coefficient of the order of $2 \times 10^{-6}$ cm³/sec.

The present results indicate that at the pressures used in the earlier work,[2,6] the ions under study were not $N_2^+$ and $O_2^+$, as had been assumed. Our preliminary value for $\alpha(N_3^+ - N_4^+)$ agrees with that reported in the earlier nitrogen work[2] and with some recent results of Van Lint et al.,[15] while our value for $\alpha(N_2^+)$ is substantially smaller, thus indicating the need for ion identification in atmospheric gas studies of this type. Studies of the recombination coefficients of other ions, such as $(NO)^+$, of importance in upper atmosphere problems, are being considered.

---

*This research has been supported in part by the Army Research Office (Durham).

†Present address: Physics Department, Thiel College, Greenville, Pennsylvania.

‡University of Pittsburgh and Westinghouse Research Laboratories, Pittsburgh, Pennsylvania.

[1]See, for example, D. R. Bates and H. S. W. Massey, Proc. Roy. Soc. (London) A187, 261 (1946); H. S. W. Massey, Advances in Physics, edited by N. F. Mott (Taylor and Francis, Ltd., London, 1952), Vol. 1,

p. 395.
[2]M. A. Biondi and S. C. Brown, Phys. Rev. 76, 1697 (1949).
[3]R. B. Holt, J. M. Richardson, B. Howland, and B. T. McClure, Phys. Rev. 77, 239 (1950).
[4]M. A. Biondi and T. Holstein, Phys. Rev. 82, 962 (1951); M. A. Biondi, Phys. Rev. 83, 1078 (1951); W. A. Rogers, Ph.D. thesis, University of Pittsburgh, 1958 (unpublished).
[5]D. R. Bates, Phys. Rev. 77, 718 (1950), and 78, 492 (1950).
[6]A. C. Faire and K. S. W. Champion, Phys. Rev. 113, 1 (1959); A. C. Faire, O. T. Fundingsland, A. L. Aden, and K. S. W. Champion, J. Appl. Phys. 29, 928 (1958).
[7]M. A. Biondi, Rev. Sci. Instr. 22, 500 (1951).
[8]R. L. F. Boyd and D. Morris, Proc. Phys. Soc. (London) 68, 1 (1955). The instruments used in the present study were manufactured by Mullard Ltd., Century House, Shaftesbury Avenue, London, England.
[9]The gases were obtained from the Matheson Company, Inc., East Rutherford, New Jersey. Undesirable impurities are less than 1 part in $10^5$.
[10]According to the observations of Faire and Champion, the recombination coefficient for electrons and nitrogen ions is constant for nitrogen pressures from 0.011 mm Hg to 4 mm Hg. It is difficult to understand this result since the present measurements yield more than an order-of-magnitude change in the relative concentrations of the various nitrogen ions over the same pressure range.
[11]The time-resolved afterglow ion currents reaching the collector of the spectrometer are small, $\sim 10^{-15}$ amp, leading to small signal/noise ratios. A modified instrument using an ion multiplier at the collector is undergoing tests.
[12]M. A. Biondi, Phys. Rev. 93, 1136 (1954).
[13]Studies of ambipolar diffusion in neon at low total pressures gave values of $D_a p \sim 450$ (cm$^2$/sec)(mm Hg) for both $N_2^+$ and $O_2^+$ ions; however, diffusion cooling effects in neon (see reference 12) caused some difficulty in these studies.
[14]E. P. Gray and D. E. Kerr, Proceedings of the Fourth International Conference on Ionization Phenomena in Gases, Uppsala, 1959 (North Holland Publishing Company, Amsterdam, 1960).
[15]V. A. J. van Lint, R. H. Hammond, and J. Parez, DASA Reaction Rate Conference, Boulder, Colorado, 1961 (unpublished).

## PHOTOPRODUCTION OF SINGLE NEUTRAL PIONS FROM HYDROGEN AT 60° IN THE 600-1100 Mev REGION

R. Diebold, R. Gomez, R. Talman, and R. L. Walker
California Institute of Technology, Pasadena, California
(Received September 20, 1961)

In a recent experiment Cortellessa and Reale[1] measured the differential cross section for the process $\gamma + p \rightarrow \pi^0 + p$ in the neighborhood of the second resonance at a center-of-mass angle for the neutral pion of 57°. Their results, obtained with a proton telescope in coincidence with a lead glass Čerenkov counter used to detect one of the $\pi^0$ decay photons, are considerably different from those which had been reported previously. Earlier data were obtained by Vette[2] using a proton magnetic spectrometer, by Stein and Rogers[3] and Worlock[4] using proton telescopes, and by DeWire, Jackson, and Littauer[5] using a proton telescope plus Čerenkov gamma-ray counter. Some of the difference can be attributed to the better resolution of Cortellessa and Reale which was ±30 Mev in incident photon energy, about half that of the previous experiments. However, even taking into account this difference in resolution, a serious disagreement exists between the experiment of Cortellessa and Reale and the earlier ones in that Cortellessa and Reale obtain values for the cross section which are, in general, considerably lower than those previously obtained. Furthermore, Cortellessa and Reale find a sharp peak in the cross section at a photon energy 700 Mev, which is about 50 Mev lower than the energy corresponding to the "second resonance" peak observed in $\pi$-nucleon scattering.[6] Although the excitation curve at any given angle need not have a maximum at the same energy as the total cross section, the angular distributions for $\pi^0$ photoproduction do not seem to be changing rapidly in this region, so that one might expect the peak at 57° to be characteristic of the total cross section and to be centered closer to 750 Mev than 700 Mev as measured by Cortellessa and Reale. (The fact that $\pi^+$ photoproduction shows a peak at 700 Mev is probably the result of an interference effect with the meson current term which does not appear in $\pi^0$ photoproduction.[7])

Intrigued by this apparent discrepancy and by the interesting shape of the curve reported by Cortellessa and Reale, we have measured the $\pi^0$ cross section in this region and extended the measurements through the third resonance using the

bremsstrahlung beam of the Caltech Synchrotron. The measurements were made by counting recoil protons alone and also by counting proton–gamma-ray coincidences. The protons were detected by a wedge-shaped, uniform field, magnetic spectrometer and associated counters.[8] They were identified both by a time-of-flight measurement and by the pulse heights in three scintillation counters located at the magnet focus. Decay photons from the $\pi^0$'s were detected in two different ways. One was by a large lead glass Čerenkov counter (30 cm high, 36 cm wide, and 36 cm deep) placed in the $\pi^0$ flight direction with the front edge 65 cm from the liquid hydrogen target. The second was by using a 1.18-cm lead converter and a scintillation counter (16 cm×20 cm) placed 60 cm from the target directly in front of the Čerenkov counter. Coincidences between the scintillator and the Čerenkov counter were then used to measure gamma rays in the smaller solid angle subtended by the lead converter. An anticoincidence counter was not used to eliminate charged particles since it was found that such a counter accidentally vetoed some $\pi^0$ events because of the numerous low-energy charged particles present. A separate measurement was made of the number of "gamma-ray" counts produced by charged particles. We did not limit the active part of the Čerenkov counter with an absorbing aperture since such an aperture would not have been well defined without an anticoincidence counter. Since the counter subtended such a large solid angle, very few of the $\pi^0$-decay $\gamma$ rays passed near its edge, and edge effects were thus quite small.

For the backward proton center-of-mass angle under investigation, it was difficult to obtain good photon energy resolution. Although we reduced the proton momentum acceptance interval to half that used by Vette, the resolution was decreased by only 20% because the angular acceptance of the magnet (±1°) contributed a great deal to the spreading of the resolution. Sizable contributions were also made by multiple scattering in the target and by slowing down in the hydrogen. Typical values of the resolution, $R(k)$ (full width at half maximum), of the experiment are: $R(585) = 70$, $R(780) = 83$, $R(1073) = 112$ Mev.

Three different counting rates were monitored and each was used separately to calculate the cross section: (1) the recoil protons alone; (2) protons in coincidence with the Čerenkov counter; (3) protons in coincidence with both the Čerenkov counter and the scintillation counter in front of the Čerenkov counter. The geometric efficiencies of the $\gamma$-ray counters were calculated using a Monte Carlo program. The Čerenkov counter was calculated to be 90% efficient at $k = 585$ Mev, increasing to 100% at $k = 731$. The geometric efficiency of the scintillation counter ranged from 52% at $k = 585$ Mev to 92% at $k = 926$. The conversion efficiency of the 1.18 cm of lead in front of the scintillation counter was estimated to be 80%.

Empty-target backgrounds of protons alone were approximately 30% of the full target counting rate. However, the Čerenkov counter coincidence requirement reduced this background to about 4%, and thus improved the counting statistics by a factor of about 1.5. Requiring both the scintillation and Čerenkov counters led to poorer statistics due to the lower efficiency for detecting the $\pi^0$ decay photons.

The set of points shown in Fig. 1 was run by varying the bremsstrahlung end point, $E_0$, with fixed kinematic settings of the spectrometer and counters corresponding to a photon energy, $k$, of 800 Mev for single $\pi^0$ photoproduction. This

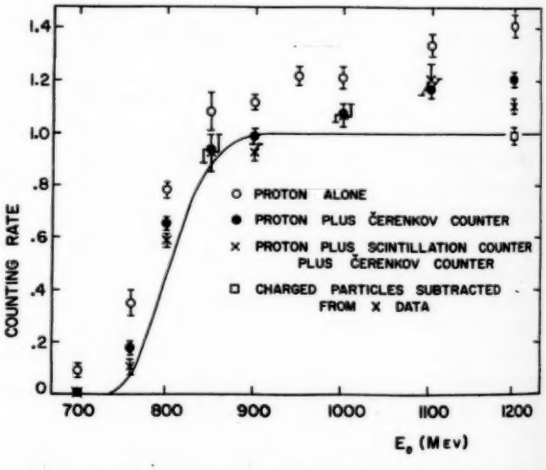


FIG. 1. Number of counts per equivalent quantum as a function of bremsstrahlung end point, $E_0$, with fixed kinematic settings of the spectrometer and counters corresponding to $k = 800$ Mev and $\theta = 60°$ c.m. for the reaction $\gamma + p \rightarrow \pi^0 + p$. Folding the resolution given by the Monte Carlo program together with the bremsstrahlung spectrum as measured by J. Boyden [Ph.D. thesis, California Institute of Technology, 1961 (unpublished)] and the cross section as measured by this experiment gives the solid line. The errors shown are those of the counting statistics only. For a given $E_0$ the errors for the three methods used are not independent.

gave a check on the resolution, on the correlation between $k$ as determined by the magnet system and $E_0$ as determined by magnetic field measurements of the synchrotron, and on the contribution from pion pairs. A comparison of the proton plus Čerenkov counter data with the calculated curve of Fig. 1 shows a discrepancy between $k$ and $E_0$ of $17 \pm 3$ Mev. Measurements at other points have indicated a similar displacement. This small discrepancy is not yet understood. The rate of rise of the experimental points for $E_0 \leq 900$ Mev agrees quite closely with that of the curve verifying the resolution calculations. The rise above $E_0 = 900$ is presumably due to pion pairs. Near the threshold for pion pairs (about 950 Mev for the equipment set at $k = 800$ Mev) the $\pi$'s come out in such a direction that most of them pass through the Čerenkov counter. To measure the charged particle contribution to the counting rate at higher $E_0$, the front scintillation counter pulse heights were examined at $E_0 = 1200$ Mev and also at 900 Mev where it was assumed that no charged particles were counted. Charged particles gave a minimum-ionizing pulse whereas the showers produced in the lead converter by the $\pi^0$ decay photons in general gave at least twice-minimum-ionizing pulses. Subtracting the charged particle contribution at 1200 Mev estimated in this way gave the point shown in Fig. 1, indicating that within the statistical accuracy of this measurement, all of the rise above 900 Mev may be ascribed to charged particles, presumably pions, counting in the Čerenkov counter.

Figure 1 also shows the extent to which cross sections obtained from the three different counting rates described above agree with each other. The counting rates of protons alone, properly normalized, were consistently higher than those with a gamma-ray coincidence. Furthermore, at $E_0 = 700$ Mev, which is below the limit of the resolution function, the proton counting rate (with empty target background subtracted) did not vanish. This indicates a background from hydrogen produced by lower energy photons. A mass-spectrograph analysis of the hydrogen showed no impurity which could account for the background. The mechanism producing these protons is not fully understood. Some of the protons probably come from particles, photoproduced by the beam, which scatter in the hydrogen (for example, $\gamma + p \rightarrow \pi^+ + n$ followed by $n + p \rightarrow n + p$). Calculations are being made to determine whether such scattering can completely explain the effect. The proton plus converted $\gamma$-ray results tend to be lower than the proton plus Čerenkov results; more detailed calculations of the lead conversion efficiency may clear up this slight discrepancy. For these reasons, the proton plus Čerenkov data are considered to be the most precise and accurate of the three sets of data.

The results of the experiment are shown in Fig. 2. Assuming a systematic error in the proton magnetic spectrometer settings of the magnitude indicated by the discrepancy shown in Fig. 1, the points were plotted at energies of approximately 2% lower than those given by the magnet settings. Empty-target backgrounds have been subtracted, and the data have been corrected for the absorption and scattering of the protons in the magnet system and for the Čerenkov geometric efficiency. Pulse-height spectra from the Čerenkov counter were measured and indicated no loss of efficiency from the electronic bias. The experiment was run with $E_0 = k + 100$ Mev, so that pion pairs were kinematically excluded and no correction was necessary. Due to the similarity of kinematics, elastic scattering of photons by protons (proton Compton effect) could not be excluded. Measurements[9] have shown this effect to be of the order of 3% of the single $\pi^0$ production. For $585 \leq k \leq 878$ Mev the points in Fig. 2 were obtained from the proton plus Čerenkov data. Above 900 Mev the Čerenkov counter was not used and the results were obtained using protons only. As a correction for the proton background from lower energy photons and processes other than $\pi^0$ production, a fixed amount, 0.31 $\mu$b/sr, was subtracted from these results (0.31 $\mu$b/sr is the average difference between the results from protons alone and the proton plus Čerenkov results; this difference was remarkably constant over the range in which the Čerenkov counter was used). Our results, while agreeing substantially with the early experiments[2-5] as typically represented by that of DeWire et al., present a much clearer picture of the second resonance. These results disagree with those of Cortellessa and Reale. The third resonance appears to be much less prominent than the second resonance and has a width comparable with that of the second resonance. The widths are not well determined because of our wide energy resolution.

Using protons alone, data are being obtained at c.m. angles 90° and 120°. The results obtained thus far show a shape at 90° similar to the one at 60°, largely agreeing with the values obtained by the early experiments once the difference in reso-

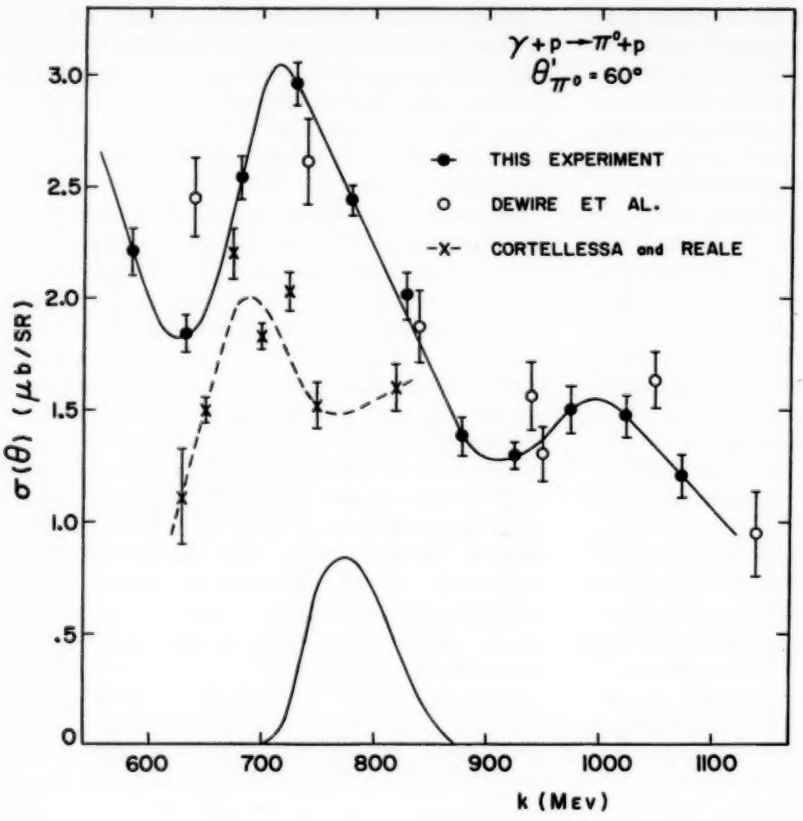


FIG. 2. Differential cross section at $\theta_\pi = 60°$ c.m. as determined by this experiment (solid circles and line) as a function of photon energy, $k$. The resolution at $k = 780$ Mev is shown at the bottom of the graph. Also shown are the cross sections obtained by Cortellessa and Reale[1] interpolated to $\theta = 60°$ (crosses and dashed line) and those of DeWire et al.[5] (open circles).

lution is taken into account.

[1]G. Cortellessa and A. Reale, Sci. Repts. Ist. Super. Sanità 1, 73 (1961); Nuovo cimento 18, 1265 (1960).

[2]J. I. Vette, Phys. Rev. 111, 622 (1958).

[3]P. C. Stein and K. C. Rogers, Phys. Rev. 110, 1209 (1958).

[4]R. M. Worlock, Phys. Rev. 117, 537 (1960).

[5]J. W. DeWire, H. E. Jackson, and Raphael Littauer, Phys. Rev. 110, 1208 (1958); Phys. Rev. 119, 1381 (1960).

[6]J. C. Brisson, J. Detoef, P. Falk-Vairant, L. van Rossum, G. Valladas, and L. C. L. Yuan, Phys. Rev. Letters 3, 561 (1959); also T. J. Devlin, B. C. Barish, W. N. Hess, V. Perez-Mendez, and J. Solomon, Phys. Rev. Letters 4, 242 (1960).

[7]A. M. Wetherell, Phys. Rev. 115, 1722 (1959).

[8]The arrangement of magnet and counters was similar to that shown in Fig. 1 of H. M. Brody, A. M. Wetherell, and R. L. Walker, Phys. Rev. 119, 1710 (1960).

[9]J. W. DeWire, M. Feldman, and R. Littauer, Proceedings of the Ninth International Annual Conference on High-Energy Physics, Rochester, New York (Interscience Publishers, Inc., New York, 1959), p. 57.

# EVIDENCE CONFIRMING THE $T=0$ THREE-PION RESONANCE*

Nguyen Huu Xuong† and Gerald R. Lynch

Lawrence Radiation Laboratory, University of California, Berkeley, California

(Received September 15, 1961)

We present here some evidence for a $T=0$, three-pion resonance with data from events of the type

$$\bar{p}+p \rightarrow 3\pi^+ + 3\pi^- + \pi^0, \qquad (1)$$

produced by antiprotons of 1.61 Bev/$c$ in the 72-in. hydrogen bubble chamber.[1] The energy and the width of the resonance agree very well with the $\omega$ meson found by Maglić et al. who analyzed the $2\pi^+ + 2\pi^- + \pi^0$ annihilations in the same experiment.[2]

We have analyzed 551 six-pronged events which are a very pure sample of six-prong pion annihilations: $\bar{p}+p \rightarrow 3\pi^+ + 3\pi^- + n\pi^0$. Of these events, $\leq 1\%$ are $\pi^- + p \rightarrow p + 3\pi^- + 2\pi^+ + n\pi^0$. Likewise, Kalbfleisch has shown that $\leq 1\%$ of these events are annihilations involving $K$ mesons.[3] When these six-pronged events were fitted by using the kinematics program KICK, 229 were found to have a $\chi^2$ less than 5.1 for reactions of type (1) and did not fit the hypothesis that no $\pi^0$ was produced. (The latter hypothesis was rejected when the $\chi^2$ for it was greater than 30.) An examination of the missing-mass distribution as well as the $\chi^2$ distribution convinces us that these 229 events contain a contamination of less than 5% of the eight-body annihilations and less than 3% of the six-body annihilations. On the other hand, roughly 10% of the true seven-body events have been excluded from the sample and are grouped with the six- and eight-body events.

We have evaluated the three-body effective mass,

$$M_3 = [(E_1+E_2+E_3)^2 - (\vec{p}_1+\vec{p}_2+\vec{p}_3)^2]^{1/2},$$

for each pion triplet in the 229 events. Each of these events yielded 33 such quantities corresponding to the charge states:

$|Q|=0$: $\pi^+\pi^-\pi^0$ (229×9 combinations),

$|Q|=1$: $\pi^\pm\pi^\pm\pi^\mp$ (229×18 combinations),

$|Q|=2$: $\pi^\pm\pi^\pm\pi^0$ (229×6 combinations).

We calculated for each value of $M_3$ an uncertainty $\delta M_3$ by using the variance-covariance matrix of the fitted-track variables, which is evaluated by KICK. The half-width, $\Gamma_{\text{resol.}}/2$, of the resolution function of $M_3$ is 9.0 Mev. However, because of systematic errors known to exist in our track reconstruction, our estimate of $\Gamma_{\text{resol.}}/2$ probably should be increased by $\sqrt{2}$ to $\Gamma_{\text{resol.}}/2 = 13$ Mev.

Figure 1 is the ideogram of the $M_3$ distribution for the 229 events. Distributions 1(a) and 1(b) are for the charge combinations $|Q|=1$ and 2, respectively. To show the difference between the neutral $M_3$ distribution and that for $|Q| \geq 1$, we have replotted at the bottom of Fig. 1 both the neutral distribution and 9/24 of the sum of the $|Q|=1$ and $|Q|=2$ distributions. This latter distribution we use as an estimate of the phase-space distribution. The neutral distribution, 1(c), shows a peak at 780 Mev that contains 76 pion

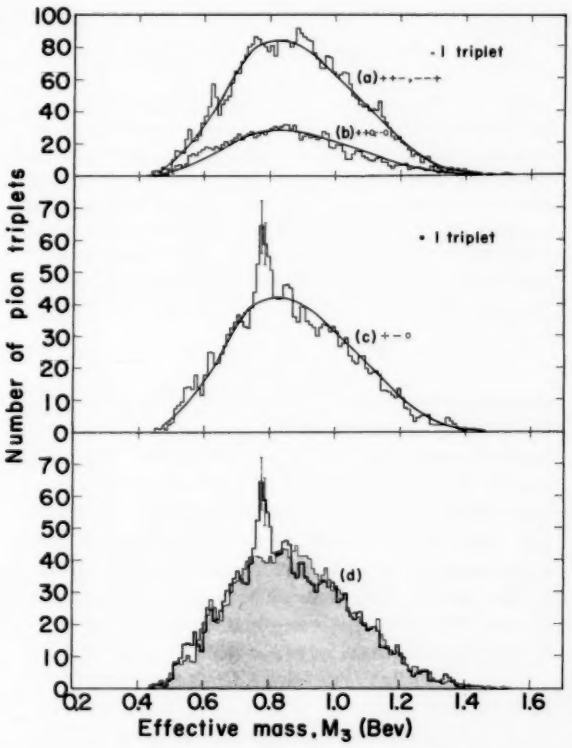


FIG. 1. Ideograms of the distributions of the effective masses ($M_3$) of pion triplets for the 229 $\bar{p}+p \rightarrow 3\pi^+ + 3\pi^- + \pi^0$ events; (a) is for the distribution for the triplets with $|Q|=1$, (b) is for triplets with $|Q|=2$, and (c) is for the triplets with $Q=0$. In (d) the combined distributions of (a) and (b) (shaded area) are compared with the (c) distribution. The same smooth curve has been drawn on (a), (b), and (c).

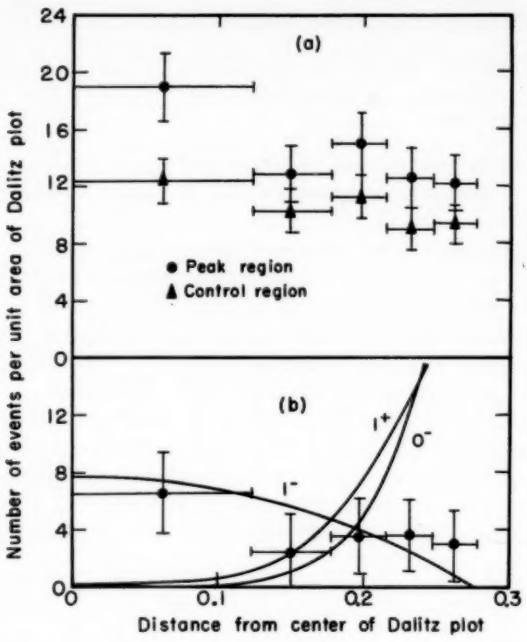


FIG. 2. The density of the population of events on the Dalitz plot for five regions of approximately equal area as a function of the average distance of this region from the center of the Dalitz plot. Both scales are in arbitrary units. (a) Events in the energy region of the $\omega$ meson and in a control region. (b) Difference between the two sets of points in (a). The three curves correspond to the predictions for this distribution on the assumptions that the particle has spin and parity $1^-$, $1^+$, or $0^-$.

triplets above a phase-space estimate of 246. Therefore, we confirm the determination of the isotopic spin of the resonance as zero. The peak has a half-width of about 18 Mev in agreement with Maglić et al.[4] We must conclude, as they did, that the half-width of the experimental peak is so close to our resolution that the true width of the peak is less than 18 Mev and could be zero. Of the 229 seven-pion annihilations, $76 \pm 18$ or $(33 \pm 8)\%$ of these proceeded via the reaction $\bar{p} + p \rightarrow \omega + 2\pi^+ + 2\pi^-$, for which the cross section is $0.6 \pm 0.15$ mb.

To determine the spin and parity of this resonance (or unstable particle), we use the method devised by Stevenson et al.,[5] who have made such a determination and conclude that the $\omega$ is a vector meson. We use events of the center of the peak (760 to 800 Mev) and events in a control region (822 to 878 Mev) of the same charge state. About 27% of the events in the peak region belong to the resonance. In Fig. 2(a), we plot the number of events per unit area of the Dalitz plot for the peak region and for the control region versus the distance from the center of the plot. The number of events per unit area of the control region is normalized to be equal to the estimated background in the peak region. Figure 2(b) shows the difference of the two sets of points in Fig. 2(a). We assume that this difference represents the number of events per unit area of the resonance.[6] These data agree very well with the curve predicted by a matrix element of a vector meson (1-) and not at all with the prediction of a pseudoscalar (0-) or axial vector meson (1+). This result of the spin and parity (1-) also agrees with that found by Stevenson et al.[5]

With the spin and parity (1-), we conclude that the $T = 0$ three-pion resonance can be the particle predicted by Nambu to explain the electromagnetic form factors of the proton and neutron,[7] and also expected in the vector-meson theory of Sakurai[8] or as a member of an octet of vector mesons, according to the unitary symmetry theory.[9] Chew has pointed out that such a vector meson can exist on dynamical grounds as a bound state.[10]

We want to thank Professor Luis Alvarez for his constant encouragement during the experiment and for his foresight and effort that made the experiment possible. We want also to thank Dr. M. Gell-Mann, Dr. B. C. Maglić, Dr. A. H. Rosenfeld, and Dr. M. L. Stevenson for many helpful discussions and advice. We wish to acknowledge the active participation of Dr. C. Tate and J. Requa in the analysis of the data. The film used in this measurement was obtained in collaboration with Dr. J. Button, Dr. P. Eberhard, Dr. G. R. Kalbfleisch, Dr. J. Lannutti, Dr. B. C. Maglić, Dr. M. Pripstein, and Dr. M. L. Stevenson; this experiment would not have been possible without their help.

---

*Work done under the auspices of the U. S. Atomic Energy Commission.

†On leave from the Viet-Nam Atomic Energy Office, Saigon, South Viet-Nam.

[1]J. Button, P. Eberhard, G. R. Kalbfleisch, J. E. Lannutti, G. R. Lynch, B. C. Maglić, M. L. Stevenson, and N. H. Xuong, Phys. Rev. 121, 1788 (1961).

[2]B. C. Maglić, L. W. Alvarez, A. H. Rosenfeld, and M. L. Stevenson, Phys. Rev. Letters 7, 178 (1961).

[3]George R. Kalbfleisch, Lawrence Radiation Laboratory Report UCRL-9597, 1961 (unpublished).

[4]The resolution for an ideogram is $\sqrt{2}$ larger than the resolution for a histogram. Thus the resolution that

should be compared with the data is $T/2 = 18$ Mev.

[5]M. L. Stevenson, L. W. Alvarez, B. C. Maglić, and A. H. Rosenfeld, Lawrence Radiation Laboratory Report UCRL-9856; Phys. Rev. (to be published). In our analysis we combined all of the data from the Dalitz plot into one graph, whereas Stevenson et al. divided the Dalitz plot into two parts.

[6]We are aware of the difficulty of making this subtraction. Some of the triplets in the peak region which are assumed to be in the background may be in $T = 0$ and exhibit the properties of the $\omega$ meson. If this is true, the background subtraction should overemphasize the effect, no matter which spin and parity the particle has.

[7]Y. Nambu, Phys. Rev. 106, 1366 (1957).

[8]J. Sakurai, Ann. Phys. 11, 1 (1960); Nuovo cimento 16, 388 (1960).

[9]M. Ikeda, S. Ogawa, and Y. Ohnuki, Progr. Theoret. Phys. (Kyoto) 22, 715 (1959). See also: Y. Ohnuki, in the Proceedings of the 1960 Annual International Conference on High-Energy Physics at Rochester (Interscience Publishers, Inc., New York, 1960); Y. Yamaguchi, Progr. Theoret. Phys. (Kyoto) Suppl. No. 11, 1, 37 (1959); J. Wess, Nuovo cimento 15, 52 (1960); Y. Neeman, Nuclear Phys. (to be published); A. Salam and J. C. Ward, Nuovo cimento 20, 419 (1961); M. Gell-Mann, Phys. Rev. (to be published); M. Gell-Mann and F. Zachariasen, Phys. Rev. (to be published); Y. Fujii, Progr. Theoret. Phys. (Kyoto) 21, 232 (1959); G. Breit, Proc. Natl. Acad. Sci. U. S. 46, 746 (1960).

[10]G. F. Chew, Phys. Rev. Letters 4, 142 (1960).